



**NAVAL
POSTGRADUATE
SCHOOL**

MONTEREY, CALIFORNIA

THESIS

**FLUID-STRUCTURE INTERACTION IN COMPOSITE
STRUCTURES**

by

Spyridon D. Plessas

March 2014

Thesis Advisor:

Second Reader:

Young W. Kwon

Joshua H. Gordis

Approved for public release; distribution is unlimited

THIS PAGE INTENTIONALLY LEFT BLANK

REPORT DOCUMENTATION PAGE			<i>Form Approved OMB No. 0704-0188</i>
Public reporting burden for this collection of information is estimated to average 1 hour per response, including the time for reviewing instruction, searching existing data sources, gathering and maintaining the data needed, and completing and reviewing the collection of information. Send comments regarding this burden estimate or any other aspect of this collection of information, including suggestions for reducing this burden, to Washington headquarters Services, Directorate for Information Operations and Reports, 1215 Jefferson Davis Highway, Suite 1204, Arlington, VA 22202-4302, and to the Office of Management and Budget, Paperwork Reduction Project (0704-0188) Washington DC 20503.			
1. AGENCY USE ONLY (Leave blank)	2. REPORT DATE March 2014	3. REPORT TYPE AND DATES COVERED Master's Thesis and Mechanical Engineer's Thesis	
4. TITLE AND SUBTITLE FLUID-STRUCTURE INTERACTION IN COMPOSITE STRUCTURES		5. FUNDING NUMBERS	
6. AUTHOR(S) Spyridon D. Plessas		8. PERFORMING ORGANIZATION REPORT NUMBER	
7. PERFORMING ORGANIZATION NAME(S) AND ADDRESS(ES) Naval Postgraduate School Monterey, CA 93943-5000		10. SPONSORING/MONITORING AGENCY REPORT NUMBER	
9. SPONSORING /MONITORING AGENCY NAME(S) AND ADDRESS(ES) N/A		11. SUPPLEMENTARY NOTES The views expressed in this thesis are those of the author and do not reflect the official policy or position of the Department of Defense or the U.S. Government. IRB Protocol number ____N/A____.	
12a. DISTRIBUTION / AVAILABILITY STATEMENT Approved for public release; distribution is unlimited		12b. DISTRIBUTION CODE	
13. ABSTRACT (maximum 200 words) In this research, dynamic characteristics of polymer composite beam and plate structures were studied when the structures were in contact with water. The effect of fluid-structure interaction (FSI) on natural frequencies, mode shapes, and dynamic responses was examined for polymer composite structures using multiphysics-based computational techniques. Composite structures were modeled using the finite element method. The fluid was modeled as an acoustic medium using the cellular automata technique. Both techniques were coupled so that both fluid and structure could interact bi-directionally. In order to make the coupling easier, the beam and plate finite elements have only displacement degrees of freedom but no rotational degrees of freedom. The fast Fourier transform (FFT) technique was applied to the transient responses of the composite structures with and without FSI, respectively, so that the effect of FSI can be examined by comparing the two results. The study showed that the effect of FSI is significant on dynamic properties of polymer composite structures. Some previous experimental observations were confirmed using the results from the computer simulations, which also enhanced understanding the effect of FSI on dynamic responses of composite structures.			
14. SUBJECT TERMS fluid-structure interaction in composite structures, finite element analysis, numerical modal analysis, experimental modal analysis, vibration mode computation, natural frequency computation.			15. NUMBER OF PAGES 99
			16. PRICE CODE
17. SECURITY CLASSIFICATION OF REPORT Unclassified	18. SECURITY CLASSIFICATION OF THIS PAGE Unclassified	19. SECURITY CLASSIFICATION OF ABSTRACT Unclassified	20. LIMITATION OF ABSTRACT UU

THIS PAGE INTENTIONALLY LEFT BLANK

Approved for public release; distribution is unlimited

FLUID-STRUCTURE INTERACTION IN COMPOSITE STRUCTURES

Spyridon D. Plessas
Lieutenant Commander, Hellenic Navy
B.S., Hellenic Naval Academy, 1996

Submitted in partial fulfillment of the
requirements for the degrees of

MECHANICAL ENGINEER

and

MASTER OF SCIENCE IN MECHANICAL ENGINEERING

from the

NAVAL POSTGRADUATE SCHOOL
March 2014

Author: Spyridon D. Plessas

Approved by: Young W. Kwon
Thesis Advisor

Joshua H. Gordis
Second Reader

Knox T. Millsaps
Chair, Department of Mechanical and Aerospace Engineering

THIS PAGE INTENTIONALLY LEFT BLANK

ABSTRACT

In this research, dynamic characteristics of polymer composite beam and plate structures were studied when the structures were in contact with water. The effect of fluid-structure interaction (FSI) on natural frequencies, mode shapes, and dynamic responses was examined for polymer composite structures using multiphysics-based computational techniques. Composite structures were modeled using the finite element method. The fluid was modeled as an acoustic medium using the cellular automata technique. Both techniques were coupled so that both fluid and structure could interact bi-directionally. In order to make the coupling easier, the beam and plate finite elements have only displacement degrees of freedom but no rotational degrees of freedom. The fast Fourier transform (FFT) technique was applied to the transient responses of the composite structures with and without FSI, respectively, so that the effect of FSI can be examined by comparing the two results. The study showed that the effect of FSI is significant on dynamic properties of polymer composite structures. Some previous experimental observations were confirmed using the results from the computer simulations, which also enhanced understanding the effect of FSI on dynamic responses of composite structures.

THIS PAGE INTENTIONALLY LEFT BLANK

TABLE OF CONTENTS

I.	INTRODUCTION.....	1
	A. MOTIVATION	1
	B. BACKGROUND AND PRIOR WORK.....	1
	1. Background	1
	2. Prior Work	2
	C. OBJECTIVES	3
	D. SUMMARY OF ORGANIZATION	3
II.	FINITE ELEMENT THEORY	5
	A. INTRODUCTION.....	5
	B. BEAM AND PLATE THEORY	5
	1. Euler-Bernoulli Beam Theory	5
	2. Analysis Technique–Computational Methods	7
	C. FLUID FINITE ELEMENT MODEL THEORY	9
	1. Introduction.....	9
	2. Fluid Domain Modeling.....	9
	D. NUMERICAL/EXPERIMENTAL MODAL ANALYSIS	10
III.	COMPOSITE BEAM FINITE ELEMENT MODEL	11
	A. VALIDATION OF THE BEAM FINITE ELEMENT MODEL.....	11
	1. Analytical, Eigenvalue, Transient Solutions.....	11
	2. Comparison of Solutions in Air	13
	B. SUMMARY OF COMPOSITE BEAM FINITE ELEMENT MODEL ...	32
IV.	COMPOSITE BEAM FEM INCLUDING FLUID-STRUCTURE INTERACTION.....	33
	A. COMPOSITE BEAM FEM CALCULATIONS	34
	1. Clamped-Clamped Beam—No Fluid-Structure Interaction	34
	2. Clamped-Clamped Beam—Fluid-Structure Interaction Included	36
	3. Natural Frequencies—No Fluid-Structure Interaction.....	37
	4. Natural Frequencies—Fluid-Structure Interaction Included	37
	B. COMPOSITE BEAM FSI FFT RESULTS FOR DIFFERENT LOADS OR INITIAL CONDITIONS	38
	1. Statics Solution as Initial Conditions without Load—With and Without FSI.....	39
	2. Statics Solution as Initial Conditions with Impulse Forcing Load—With and Without FSI.....	41
	3. Zero Displacement as Initial Conditions with Impulse Forcing Load—With and Without FSI.....	41
	4. Mode 1 Displacement as Initial Conditions without Load—With and Without FSI.....	43
	5. Mode 1 Displacement as Initial Conditions with Impulse Forcing Load—With and Without FSI.....	44

6.	Mode 2 Displacement as Initial Conditions without Load— With and Without FSI.....	45
7.	Mode 2 Displacement as Initial Conditions with Impulse Forcing Load—With and Without FSI.....	47
8.	Mode 3 Displacement as Initial Conditions without Load— With and Without FSI.....	47
9.	Mode 2 Displacement as Initial Conditions with Impulse Forcing Load—With and Without FSI.....	49
C.	SUMMARY OF COMPOSITE BEAM FEM INCLUDING FSI.....	49
V.	COMPOSITE PLATE FINITE ELEMENT MODEL INCLUDING FLUID- STRUCTURE INTERACTION	51
A.	3D COMPOSITE-PLATE FINITE ELEMENT MODEL.....	51
B.	RESULTS OF PLATE FEM CALCULATION INCLUDING FSI.....	52
1.	Statics Solution (Produced by Forcing Load) as Initial Conditions without Applied Load	52
2.	Zero Displacement as Initial Conditions with Impact Forcing Load—With and Without FSI.....	58
3.	Statics Solution (Produced by Moment Load) as Initial Conditions—With and Without FSI	65
C.	SUMMARY OF PLATE FEM INCLUDING FSI.....	72
VI.	CONCLUSIONS AND RECOMMENDATIONS.....	75
A.	SUMMARY OF CONCLUSIONS	75
B.	RECOMMENDATIONS FOR FUTURE WORK.....	76
	LIST OF REFERENCES	79
	INITIAL DISTRIBUTION LIST	81

LIST OF FIGURES

Figure 1.	Beam FEM Displacement Only dof, from [2], [3].....	7
Figure 2.	Plate FEM Displacement Only dof, from [2].....	8
Figure 3.	Cantilever Beam Using Ten Elements—Mode 1.....	14
Figure 4.	Cantilever Beam Using Ten Elements—Mode 2.....	15
Figure 5.	Cantilever Beam Using Ten Elements—Mode 3.....	15
Figure 6.	Cantilever Beam Using 20 Elements—Mode 1.....	16
Figure 7.	Cantilever Beam Using 20 Elements—Mode 2.....	17
Figure 8.	Cantilever Beam Using 20 Elements—Mode 3.....	17
Figure 9.	Cantilever Beam Using 40 Elements—Mode 1.....	18
Figure 10.	Cantilever Beam Using 40 Elements—Mode 2.....	19
Figure 11.	Cantilever Beam Using 40 Elements—Mode 3.....	19
Figure 12.	Pinned-Pinned Beam Using Ten Elements—Mode 1.....	20
Figure 13.	Pinned-Pinned Beam Using Ten Elements—Mode 2.....	21
Figure 14.	Pinned-Pinned Beam Using Ten Elements—Mode 3.....	21
Figure 15.	Pinned-Pinned Beam Using 20 Elements—Mode 1.....	22
Figure 16.	Pinned-Pinned Beam Using 20 Elements—Mode 2.....	23
Figure 17.	Pinned-Pinned Beam Using 20 Elements—Mode 3.....	23
Figure 18.	Pinned-Pinned Beam Using 40 Elements—Mode 1.....	24
Figure 19.	Pinned-Pinned Beam Using 40 Elements—Mode 2.....	25
Figure 20.	Pinned-Pinned Beam Using 40 Elements—Mode 3.....	25
Figure 21.	Clamped-Clamped Beam Using Ten Elements—Mode 1.....	26
Figure 22.	Clamped-Clamped Beam Using Ten Elements—Mode 2.....	27
Figure 23.	Clamped-Clamped Beam Using Ten Elements—Mode 3.....	27
Figure 24.	Clamped-Clamped Beam Using 20 Elements—Mode 1.....	28
Figure 25.	Clamped-Clamped Beam Using 20 Elements—Mode 2.....	29
Figure 26.	Clamped-Clamped Beam Using 20 Elements—Mode 3.....	29
Figure 27.	Clamped-Clamped Beam Using 40 Elements—Mode 1.....	30
Figure 28.	Clamped-Clamped Beam Using 40 Elements—Mode 2.....	31
Figure 29.	Clamped-Clamped Beam Using 40 Elements—Mode 3.....	31
Figure 30.	Clamped-Clamped Beam—Mode 1 without FSI.....	35
Figure 31.	Clamped-Clamped Beam—Mode 2 without FSI.....	35
Figure 32.	Clamped-Clamped Beam—Mode 1 with FSI.....	36
Figure 33.	Clamped-Clamped Beam—Mode 2 with FSI.....	36
Figure 34.	FFT of Displacement, without FSI.....	39
Figure 35.	FFT of Displacement, with FSI.....	40
Figure 36.	FFT of Displacement, without FSI.....	42
Figure 37.	FFT of Displacement, with FSI.....	42
Figure 38.	FFT of Displacement, without FSI.....	43
Figure 39.	FFT of Displacement, with FSI.....	44
Figure 40.	FFT of Displacement, without FSI.....	45
Figure 41.	FFT of Displacement, with FSI.....	46
Figure 42.	FFT of Displacement, without FSI.....	48

Figure 43.	FFT of Displacement, with FSI.	48
Figure 44.	Mesh of the 12X12 3D FEM Plate.	52
Figure 45.	Initial Conditions of 3D Plate for this Case.	53
Figure 46.	Overall Surface of Deformed Plate, without FSI.	53
Figure 47.	Overall Surface of Deformed Plate, with FSI.	54
Figure 48.	Deformed Plate, without FSI.	55
Figure 49.	Deformed Plate, with FSI.	55
Figure 50.	Mode One, without FSI.	56
Figure 51.	Mode One, with FSI.	56
Figure 52.	FFT of Displacement, without FSI.	57
Figure 53.	FFT of Displacement, with FSI.	57
Figure 54.	Deformed Plate, without FSI.	59
Figure 55.	Deformed Plate, with FSI.	59
Figure 56.	Displacement of Central Node, without FSI.	60
Figure 57.	Displacement of Central Node, with FSI.	60
Figure 58.	FFT of Displacement, without FSI.	61
Figure 59.	FFT of Displacement, with FSI.	61
Figure 60.	Mode One, without FSI.	62
Figure 61.	Mode One, with FSI.	62
Figure 62.	Mode One Difference, without-with FSI.	63
Figure 63.	Second Symmetric Mode, without FSI.	63
Figure 64.	Second Symmetric Mode, with FSI.	64
Figure 65.	Second Symmetric Mode Difference, without-with FSI.	64
Figure 66.	Initial Conditions for this Case.	65
Figure 67.	Deformed Plate, without FSI.	66
Figure 68.	Deformed Plate, with FSI.	66
Figure 69.	Displacement at Center Node, without FSI.	67
Figure 70.	Displacement at Center Node, with FSI.	67
Figure 71.	FFT of Displacement, without FSI.	68
Figure 72.	FFT of Displacement, with FSI.	68
Figure 73.	Mode Shape, without FSI.	69
Figure 74.	Mode Shape, with FSI.	69
Figure 75.	Mode Shape Difference, without-with FSI.	70
Figure 76.	Mode Shape, without FSI.	71
Figure 77.	Mode Shape, with FSI.	71
Figure 78.	Mode Shape Difference, without-with FSI.	72

LIST OF TABLES

Table 1.	Natural Frequencies Using Ten Finite Elements in Air.....	14
Table 2.	Cantilever Beam Using 20 Elements—Natural Frequencies for the First Five Modes in Air.	16
Table 3.	Cantilever Beam Using 40 Elements—Natural Frequencies for the First Five Modes in Air.	18
Table 4.	Pinned-Pinned Beam Using Ten Elements—Natural Frequencies for the First Five Modes in Air.....	20
Table 5.	Pinned-Pinned Beam Using 20 Elements—Natural Frequencies for the First Five Modes in Air.....	22
Table 6.	Pinned-Pinned Beam Using 40 Elements—Natural Frequencies for the First Five Modes in Air.....	24
Table 7.	Clamped-Clamped Beam Using 10 Elements—Natural Frequencies for the First Five Modes in Air.....	26
Table 8.	Clamped-Clamped Beam Using 20 Elements—Natural Frequencies for the First Five Modes in Air.....	28
Table 9.	Clamped-Clamped Beam Using 40 Elements—Natural Frequencies for the First Five Modes in Air.....	30
Table 10.	Natural Frequencies without FSI.	37
Table 11.	Comparison of Natural Frequency with and without FSI for Impulse Load. ..	38
Table 12.	Comparison of Natural Frequency with and without FSI for Static Initial Displacement.....	40
Table 13.	Comparison of Natural Frequency with and without FSI for Impulse Load and Statics Displacement.	41
Table 14.	Comparison of Natural Frequency with and without FSI for Mode 1 Initial Displacement.....	44
Table 15.	Comparison of Natural Frequency with and without FSI for Mode 1 Initial Displacement with Impulse Load.	45
Table 16.	Comparison of Natural Frequency with and without FSI for Mode 2 Initial Displacement.....	46
Table 17.	Comparison of Natural Frequency with and without FSI for Mode 2 Initial Displacement with Impulse Load.	47
Table 18.	Comparison of Natural Frequency with and without FSI for Mode3 Initial Displacement.....	49
Table 19.	Comparison of Natural Frequency with and without FSI for Mode 3 Initial Displacement with Impulse Load.	49

THIS PAGE INTENTIONALLY LEFT BLANK

LIST OF ACRONYMS AND ABBREVIATIONS

1D	one-dimensional
2D	two-dimensional
3D	three-dimensional
CA	cellular automata
CG	continuous Galerkin's method
DFT	Discrete Fourier Transform
DG	discontinuous Galerkin's method
dof	degree(s) of freedom
EOM	equations of motion
FEA	finite element analysis
FE	finite element
FEM	finite element method
FFT	Fast Fourier Transform
FSI	Fluid-Structure Interaction
IVP	initial value problem
PDE	partial differential equation
SS	Simply Supported

THIS PAGE INTENTIONALLY LEFT BLANK

ACKNOWLEDGMENTS

I would like to thank my wife, Ioulia Moscholiou, and my kids, Dionysios and Konstantina, for their infinite patience, understanding, and their tremendous support of my endeavor, before and during my time in the NPS.

I would also like to thank my parents, my in-laws, and my family for their important role of enlightening me with the spirit of persistency and hard work.

My special appreciation and thank you to:

- Distinguished Professor Young W. Kwon for his tremendous support, excellence in teaching, and the vast amount of knowledge that he freely and without hesitation offered to me throughout my time in NPS. His talented and outstanding performance as a professor, instructor, scientist and friend boosted my level of understanding, my interest, and my performance in all academic levels and subjects and especially in my thesis topic. He helped me more than any other to overcome every difficulty that arose.
- Associate Professor Joshua H. Gordis for his excellent professionalism and outstanding teaching ability. He enabled me to deeply understand difficult subjects that played a significant role in my MAE studies in NPS. I want to thank him for his support, knowledge, and help that he gave me.
- The Hellenic Navy that believed in me being able to acquire the Master of Science Degree and the Mechanical Engineer Degree. The knowledge that I have acquired will definitely help me as an officer to improve, upgrade, strongly support, and sustain our navy's role as the superior naval force in our homeland region of the world.

Especially, I want to thank Hellenic Navy officer and NPS-MAE Aeronautical Engineer George P. Christopoulos, who inspired, motivated, supported, and believed in me at the times when all this was just a dream.

THIS PAGE INTENTIONALLY LEFT BLANK

I. INTRODUCTION

A. MOTIVATION

Composite materials are of great interest currently as they prove to have many significant advantages over the “traditional” materials in shipbuilding, marine, and aerospace industry applications. In particular, they possess many beneficial, useful, and practical properties, which include, but are not limited to, their superior strength and stiffness compared to their density and weight, their excellent resistance to corrosion and marine environmental deterioration, and their ability to be built in almost any shape that the designer wishes to make.

Composite structures are currently used in many military and civilian applications. But a rise in interest in composites is expected to occur in the near future, as their lightweight but strong and stiffer characteristics make them among the most suitable primary materials for use in building fuel-efficient and therefore cost-efficient naval ships, vessels, and marine structures.

B. BACKGROUND AND PRIOR WORK

1. Background

The Finite Element Method (FEM) is a well-proven method to study, model, and predict the response of a structure when loads (moments or forces) are applied. A great amount of research has been made using the FEM to study and simulate the cases when the structures are surrounded by air. But there is still much to be explored in the case where the structure is surrounded by fluid. The most interesting case is when it is surrounded by water, as this is usually the case when composite structures are being used for building sea vessels or in similar applications like small, fast-attack Navy ships, mine-hunters, mine-sweepers, auxiliary Navy vessels, motorboats, and unmanned aerial, underwater or surface vehicles.

The procedure of experimental testing of composite structures to capture their response and dynamic vibrational characteristics is an expensive and relatively inefficient

method. The reason is that most of the initial conditions that we wish to actually apply to the structure cannot be physically and accurately implemented. For example, imposing initial conditions of mode shape #3 onto a clamped-clamped composite beam cannot be practically feasible. It cannot be represented accurately enough in order to be used as initial conditions.

But when it comes to computational methods in mechanical engineering, like the finite element method, it is easier to simulate almost any initial condition while the only requirement is that the finite element model accurately represents the structure and its behavior. In this thesis, a series of studies has been carried out in order to validate our finite element models and to actually verify that the results are reasonable and truthful, and that they match the theoretical analytically predicted, as well as match the results from related experiments.

Therefore, the advantages of calculating the structure's response computationally rather than experimentally are tremendous, and they definitely allow us to re-design and optimize the structure before it is actually built and experimentally tested. This way the total effort of designing or optimizing a composite structure proves to be faster and cheaper than actually building many experimental subjects and their iterations.

2. Prior Work

Significant progress in research associated with the FEM in structures made from composites has been made by Y. W. Kwon and L. E. Craugh [1], who have developed, validated, and tested the FEM of a plate subject to forcing load while investigating the development of a crack.

Their work utilized discontinuous Galerkin's method for solving boundary value problems. This approach is beneficial since it has the concept of weak enforcement of continuity between elements, and applies it to elliptic problems. The 'relaxed' continuity requirements in between the elements possess many advantages to the methodology since the calculations can be carried out taking advantage of the parallel-threading computer architecture. Moreover, each element is not dependent on the other, which allows us to

use different types and orders of interpolation throughout the structure for easier meshing.

The increasing use of composite technology in maritime applications requires further work examining the mass effects imparted to composite structures in contact with a fluid environment. In particular, evaluation of damage and residual strength are necessary for a proper evaluation of the survivability potential of a proposed design.

C. OBJECTIVES

The objective of this research was to investigate dynamic characteristics of polymer composite beam and plate structures when the structures were in contact with water. The effect of fluid-structure interaction (FSI) on natural frequencies, mode shapes, and dynamic responses was examined for polymer composite structures using multiphysics-based computational techniques. Composite structures were modeled using the finite element method. The fluid was modeled as an acoustic medium using the cellular automata technique. Both techniques were coupled so that both fluid and structure could interact bi-directionally. The fast Fourier transform (FFT) technique was applied to the transient responses of the composite structures with and without FSI, respectively, so that the effect of FSI can be examined by comparing the two results.

D. SUMMARY OF ORGANIZATION

This thesis consists of the following chapters: Chapter II is a short reference to the Beam and Plate Theory on which the Finite Element Model was based. The mathematical formulation which was the base of the development and implementation of the finite element model is also presented and justified in this chapter. A description of the coupling between the fluid FEM solutions to the dynamic structural solution is also presented. Chapter III contains the characteristics, the setup, and the validation of the composite beam FEM used in this thesis. Chapter IV includes the FEM results including fluid-structure interaction for the composite beam. Chapter V contains a description of the characteristics, the setup, and the validation methods of the 3D FEM for the composite plate. Chapter VI contains the FEM results, including the fluid-structure interaction for the 3D FEM composite plate. Finally, Chapter VII includes a summary of

the conclusions of this research and the recommendations for future research efforts in this subject.

II. FINITE ELEMENT THEORY

A. INTRODUCTION

Beams and plates are very interesting since they are very commonly used in most structures as they are remarkably efficient when loaded. They are considered to be the fundamental parts of almost any structure.

The partial differential equations (PDEs) are derived from setting up the equations of motion (EOM) of the beam and plate. The approach of the Finite Element Analysis combines the geometry and constraints of the structure with the material properties of its components to generate a response (e.g., displacement, stress, and/or strain) to some specific known loading.

For the sake of simpler calculations the structure is ‘discretized’ and ‘represented’ from a collection of smaller structure-pieces (or domains) that are called ‘finite elements’. The geometry of the finite elements is much simpler to be represented from a mathematical expression, than the actual continuous structure. This simpler mathematical expression is used to solve each finite element, and the total solution of the whole structure is derived as the simultaneous solution of all finite element. The global solution is subject to solid requirements of structural integrity and compatibility and also implementing boundary conditions.

The finite element formulation used to represent these structures is presented and analyzed along with the finite element formulation used to represent the fluid, which in this study is water.

B. BEAM AND PLATE THEORY

1. Euler-Bernoulli Beam Theory

The finite element model we developed is based on the Euler-Bernoulli beam theory. According to this theory the equation for beam bending is the following:

$$\rho \frac{\partial^2 u}{\partial t^2} + \frac{\partial^2}{\partial x^2} \left(EI \frac{\partial^2 u}{\partial x^2} \right) = q(x, t) \quad (2.1)$$

where $u(x,t)$ is the transverse displacement of the beam, ρ is the mass density per unit length, EI is the beam rigidity, $q(x,t)$ is the pressure load, t is the time variable, and x is the spatial variable along x -axis.

The finite element mathematical formulation is developed by applying a method of weighted residual, the Galerkin's method, to the partial differential equation of the beam bending Eqn. (2.1). The method of weighted residual for the PDE in Eqn. (2.1) gives the following integral equation, assuming that L is the beam's length and w is a test function:

$$I = \int_0^L \left(\rho \frac{\partial^2 u}{\partial t^2} + \frac{\partial^2}{\partial x^2} \left(EI \frac{\partial^2 u}{\partial x^2} \right) - q \right) w dx = 0 \quad (2.2)$$

We now apply integration by parts of the second term of this integral equation twice and we get Equation (2.3):

$$I = \sum_{i=1}^n \left[\int_{\Omega^e} \rho \frac{\partial^2 u}{\partial t^2} w dx + \int_{\Omega^e} EI \frac{\partial^2 u}{\partial x^2} \frac{\partial^2 w}{\partial x^2} dx - \int_{\Omega^e} q w dx \right] + \left[-Vw - M \frac{\partial w}{\partial x} \right]_0^L = 0 \quad (2.3)$$

where the shear force is:

$$V = -EI \left(\frac{\partial^3 u}{\partial x^3} \right) \quad (2.4)$$

The bending moment is:

$$M = EI \left(\frac{\partial^2 u}{\partial x^2} \right) \quad (2.5)$$

The element domain is Ω^e , and the number of the finite elements of the beam is n . This equation implements the discretization of the beam to an n -number of finite elements.

The Euler-Bernoulli beam theory is based on the assumption that the plane normal to the neutral axis before the deformation will still remain normal to the neutral axis after deformation. The slope at each node is the first derivative of the vertical deflection with

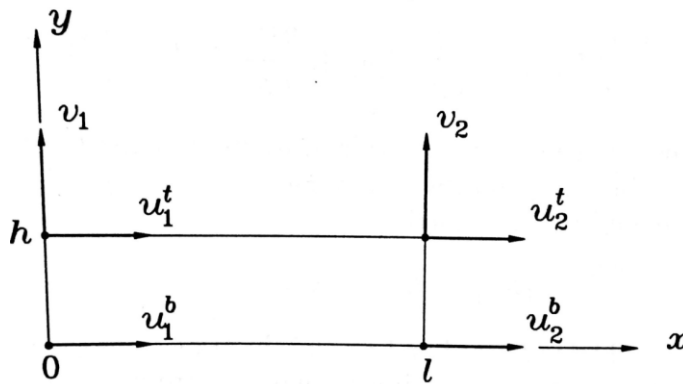
respect to x , i.e. $\theta = \frac{dv}{dx}$. We choose the shape functions such that they can represent—by spatial interpolation—the transverse deflection of the beam at each nodal point location.

2. Analysis Technique–Computational Methods

The ‘time-marching’ technique was used to produce the solutions over time. That means that we solved both structural FEM and fluid models for one time instant, i.e. the ‘time step.’ Then, this solution was set to be the initial condition for the next time step. In particular, the solution for the structural FEM was produced and it was ‘fed’ to the cellular automata fluid domain as initial conditions. Then, the ‘return’ solution of the cellular automata was ‘fed’ to the structural FEM as initial conditions in order to start the next computation at the following time step. Special care was given to the length of the time step, since if it was not chosen carefully the iterative method either diverged from or the phenomenon ended before the FEM was able to ‘capture’ the structure’s response.

a. Finite Element Analysis Beam Model

The finite element model of the beam was developed to have displacement degrees of freedom (dof) only. It takes account of the thickness of the element and it can capture the behavior with respect to the deformation along the dimension of the thickness. The finite element that we used to represent the 2D composite beam in our FEM program is shown in Figure 1. .



Four-Noded Beam Element with Six Degrees of Freedom

Figure 1. Beam FEM Displacement Only dof, from [2], [3].

b. Finite Element Analysis Plate Model

The finite element model of the plate was constructed to have only displacement dof. This has a significant advantage over the rotational dof. It can take account of the thickness of the element, and it can easily separate fluid at the bottom and top sides of the plate. The displacement dof-only finite element that we used to represent the 3D plate is shown in Figure 2. .

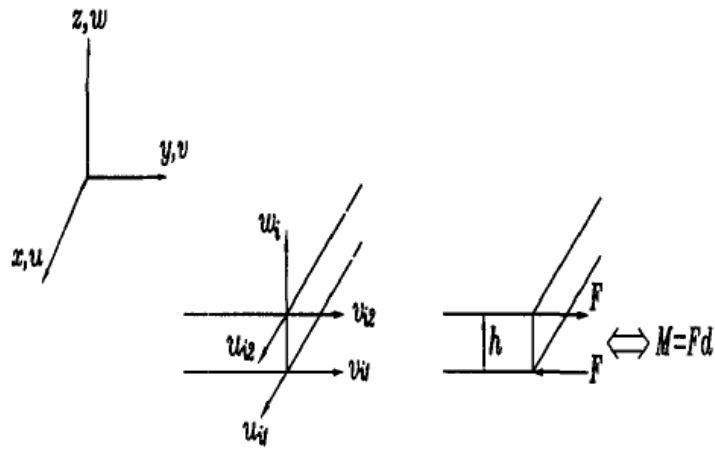


Figure 2. Plate FEM Displacement Only dof, from [2].

C. FLUID FINITE ELEMENT MODEL THEORY

1. Introduction

The fluid model was modeled as an acoustic medium. It was assumed to be stationary. Fluid flow has not been taken into account in this study. Instead, a velocity potential of the fluid in the field was the way that the fluid-structure interaction was analyzed. The transverse velocity of the composite structure (beam or plate) was matched to the velocity of the fluid along the z -axis in order to satisfy the compatibility requirement. Therefore, the fluid analysis has only the essential information and solutions that are needed for the scope of observing the FSI effects on the structure and not as a detailed fluid analysis.

2. Fluid Domain Modeling

We assume that ϕ is the velocity potential of the fluid, \vec{v} the fluid velocity, c the speed of sound in the fluid medium. From the definition of the velocity potential of the fluid we have:

$$\vec{v} = \nabla \phi \quad (2.6)$$

The wave equation was used to simulate the propagation of the fluid disturbance across the fluid medium:

$$\ddot{\phi} = c^2 \nabla^2 \phi \quad (2.7)$$

We chose the fluid domain as a domain with non-reflecting boundary conditions and used cellular automata to model the acoustic field.

The basic idea behind the cellular automata technique is that the fluid domain is divided into a grid of fixed-size cells. Each cell has certain values associated with it to represent its state. The values that are ‘held’ in cells are water density, velocity potential, location, and its location. Every cell is updated every iteration based on the state of its neighboring cells. Differences between them result in changes to the state of the cell according to the specified rule. That is how the solution of each cell of the fluid domain is obtained. Then, this solution is ‘fed’ back to the structural model and is set as the compatibility condition for the finite element model.

D. NUMERICAL/EXPERIMENTAL MODAL ANALYSIS

Modal analysis is defined as a process with which we describe a structure in terms of its modal parameters. These are the mode shapes, the natural frequencies, the damping ratios, etc. Modal analysis is the study of the dynamic character of a system which is defined independently from the loads applied to it and the system's response. Structural dynamics is the study and analysis of how structures respond when they are subjected to applied loads. In our research the modal characteristics of the structure were used to determine the response of the system.

The experimental data from fluid-structure interaction tests are processed using the experimental modal analysis technique to extract useful information of the response of the test sample. In our case where the FEM model is a mathematical model which is computationally simulated, we used numerical modal analysis in order to extract useful information, i.e. mode shapes, natural frequencies, deflections, etc. from the numerical data. That means that we treated the numerical results/solutions of the FEM calculations as experimental data in order to 'derive' the structure's dynamic response.

In the case where the excitation caused by the applied load is the same as a vibration mode, then that mode is excited; otherwise, the response is the linear combination or the sum of all the excited modes.

As is the usual practice in analyzing experimental data sets, we used the exact same technique, the FFT, in order to analyze the numerical 'data sets' produced by our finite element program. The FFT was applied to the numerical 'data' that were produced by our finite element model. We treated this numerical data the same way as if they were experimental data. We applied the fast FFT technique and the results were interpreted in order to obtain an appreciation and an understanding of the dynamic properties of the response of the structure.

III. COMPOSITE BEAM FINITE ELEMENT MODEL

A. VALIDATION OF THE BEAM FINITE ELEMENT MODEL

The finite element model that was developed has been validated for consistency of results. This was achieved by comparing the results of the transient FEM analysis with FFT to the analytical (exact) and the FEM eigenvalue solutions. The FFT technique was applied to the transient FEM solution, such as nodal displacements, velocities, and/or accelerations, so as to compute natural frequencies and mode shapes of beams. Then, the results were compared to the solutions obtained from the eigenvalue analysis using the FEM as well as analytical solutions. The aforementioned calculation and comparison were done for the cases of clamped-clamped, cantilever, and simply-supported beams. We chose the beam to be of a composite material of length 1.0 m, thickness 0.05 m, width 0.1 m, Young's modulus of elasticity $E=20 \times 10^9$ Pa, density 2000 Kg/m^3 and Poisson's ratio 0.3. The results of each case are provided in the following sections.

1. Analytical, Eigenvalue, Transient Solutions

a. Analytical/Exact Solutions

(1) Eigenvalue Solution of a Cantilever Beam. The equation that we used in order to compute the eigenvalue solution for the composite cantilever beam was:

$$\phi(x) = A(\cos \beta x - \cosh \beta x) + (\sin \beta x - \sinh \beta x) \quad (3.1)$$

where

$$A = -\frac{\sin \beta l + \sinh \beta l}{\cos \beta l + \cosh \beta l} \quad (3.2)$$

and l is the overall length of the beam, x is the distance from the root of the beam, and $\beta l = 1.875104$ for Mode 1, $\beta l = 4.694091$ for Mode 2, $\beta l = 7.854757$ for Mode 3.

(2) Eigenvalue Solution of a Pinned-Pinned Beam. The equation that we used in order to compute the eigenvalue solution for the composite pinned-pinned beam was:

$$\phi(x) = A \sin \beta x \quad (3.3)$$

where

$$A = \frac{\cosh \beta l}{\cos \beta l} \quad (3.4)$$

and l is the overall length of the beam, x is the distance from the end of the beam, and $\beta l = 3.141593$ for Mode 1, $\beta l = 6.283185$ for Mode 2, $\beta l = 9.424778$ for Mode three.

(3) Eigenvalue Solution of a Clamped-Clamped Beam. The equation that we used in order to compute the eigenvalue solution for the composite clamped-clamped beam was the same as Eq. (3.1) where

$$A = -\frac{\sin \beta l - \sinh \beta l}{\cos \beta l - \cosh \beta l} \quad (3.5)$$

b. FEM Transient Solution

This technique is similar to the experimental modal analysis. In the experimental modal analysis, an impulse load is applied to a specimen and the response of the specimen is obtained from sensors such as accelerometers. Then, the data from the sensors are processed using the fast Fourier transform (FFT) technique. In this study, the transient responses were calculated from the FEM program we developed by applying an impulse load or non-zero initial conditions. Then, the use of FFT allowed us to filter and capture the behavior of the structure (i.e., the dynamic response), and exploit the mode shapes and the natural frequencies.

The implementation of the FFT algorithm was conducted by using the function ‘fft’ which is embedded in MATLAB. Special caution was used to choose the appropriate time step Δt so that the FFT algorithm had the necessary ‘resolution’ to capture the response of the structure. If the time step Δt was ‘too large,’ then the FFT algorithm could not show the transient response. When the time step Δt was too small, the computational cost of the FFT algorithm increased significantly.

As stated in [3], the requirement for Δt is to be smaller or equal to $\Delta t_{crit} = \frac{T_{min}}{\pi}$ in order for the central difference method algorithm to be conditionally stable. This central difference method algorithm was used for numerical differentiation of the displacement and velocity of the nodal points in order to compute the velocity from the displacement and the acceleration from the velocity.

c. Eigenvalue Analysis

Using the finite element method, the mass and stiffness matrices are computed for the beam structures. Then, eigenvalue analysis is undertaken with the following equation

$$(\mathbf{K} - \lambda_i \mathbf{M})\phi_i = 0 \quad (3.6)$$

where \mathbf{K} and \mathbf{M} are the stiffness and mass matrices, λ_i and ϕ_i is the i -th eigenvalue and eigenvector. The eigenvalue is the square of the circular natural frequency while the eigenvector represents the mode shape.

2. Comparison of Solutions in Air

The solution of each method discussed in the previous paragraphs was calculated, and the resulting mode shapes and natural frequencies are then plotted and tabulated respectively for validation of our FEM program.

a. Comparison of Solutions for Cantilever Beam Using Ten Finite Elements

Figure 3. through Figure 5. compare the first three mode shapes of a cantilever beam using ten elements. Table 1. compares the first five natural frequencies.

Cantilever 10 Elements	Natural Frequency Exact Solution	Natural Frequency Eigenvalues Solution	Natural Frequency Transient Solution
Mode 1	25.54	25.54 (0 %)	27.30 (6.49 %)
Mode 2	160.06	160.07 (0.006 %)	169.00 (6.20 %)
Mode 3	448.19	448.30 (0.024 %)	480.00 (7.09 %)
Mode 4	878.27	879.10 (0.113 %)	940.00 (7.028 %)
Mode 5	1,451.85	1,455.51 (0.252 %)	1,560.00 (7.449%)

Table 1. Natural Frequencies Using Ten Finite Elements in Air.

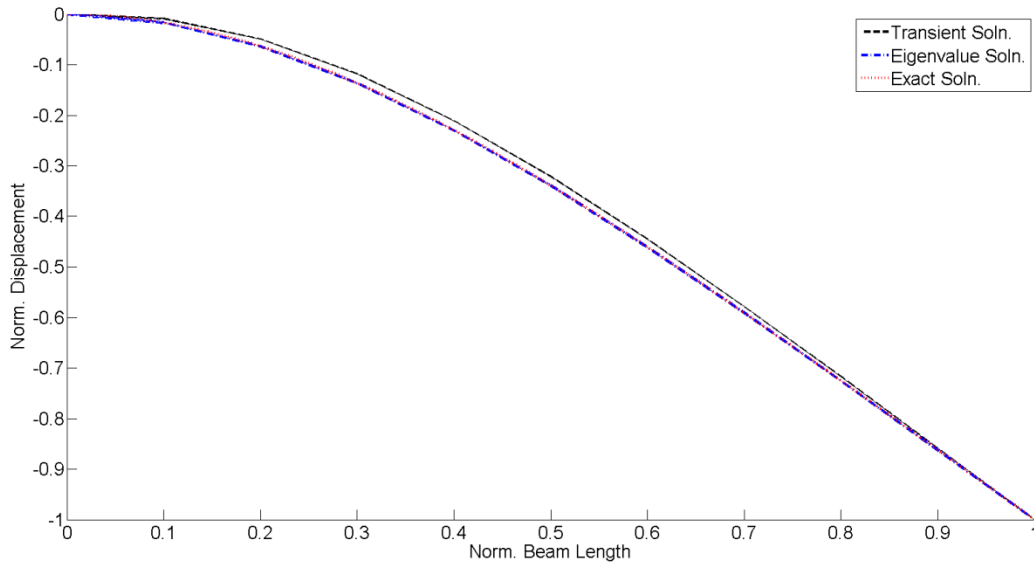


Figure 3. Cantilever Beam Using Ten Elements—Mode 1.

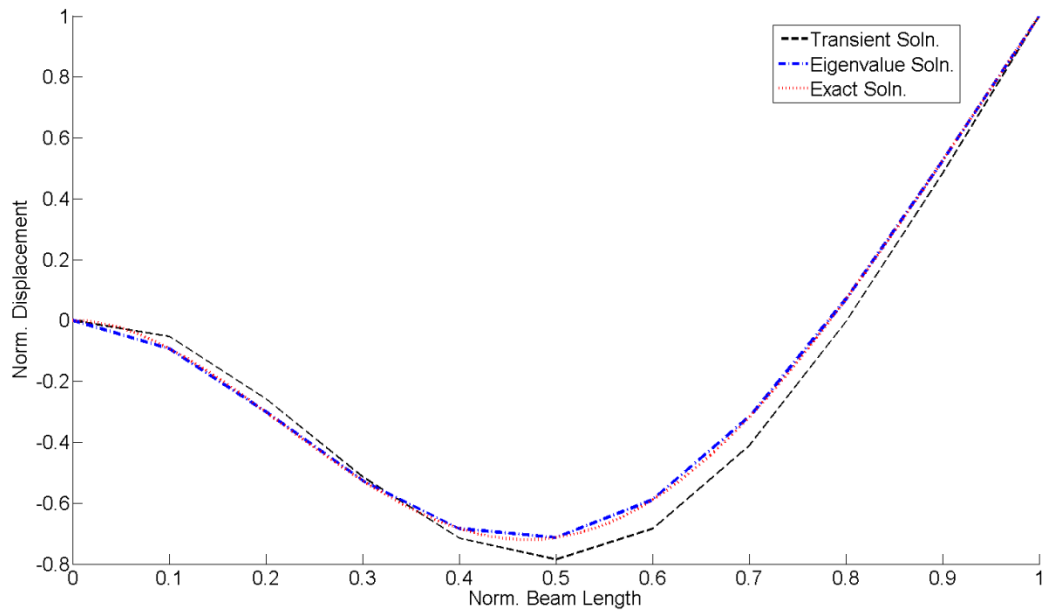


Figure 4. Cantilever Beam Using Ten Elements—Mode 2.

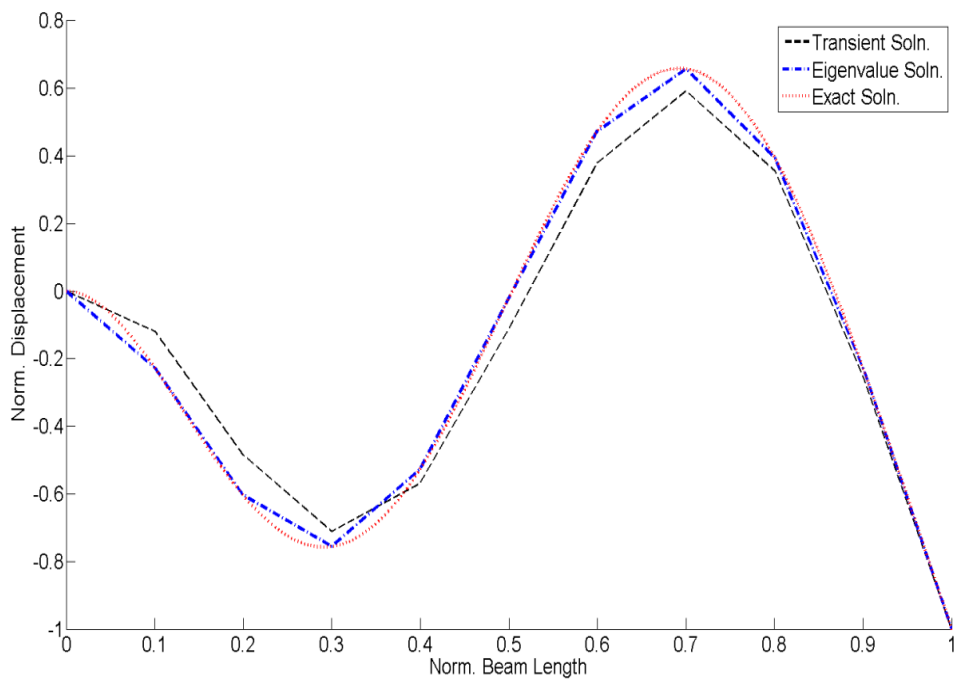


Figure 5. Cantilever Beam Using Ten Elements—Mode 3.

b. Comparison of Solutions for Cantilever Beam Using 20 Finite Elements

Figure 6. through Figure 8. compare the first three mode shapes of a cantilever beam using 20 elements. Table 2. compares the first five natural frequencies.

Cantilever 20 Elements	Natural Frequency Exact Solution	Natural Frequency Eigenvalues Solution	Natural Frequency Transient Solution
Mode 1	25.54	25.54 (0 %)	26.70 (4.54 %)
Mode 2	160.06	160.06 (0 %)	170.00 (6.21 %)
Mode 3	448.19	448.20 (0.002 %)	460.00 (2.63 %)
Mode 4	878.27	878.33 (0.006 %)	910.00 (3.61 %)
Mode 5	1451.85	1452.10 (0.017 %)	1500.00 (3.31 %)

Table 2. Cantilever Beam Using 20 Elements—Natural Frequencies for the First Five Modes in Air.

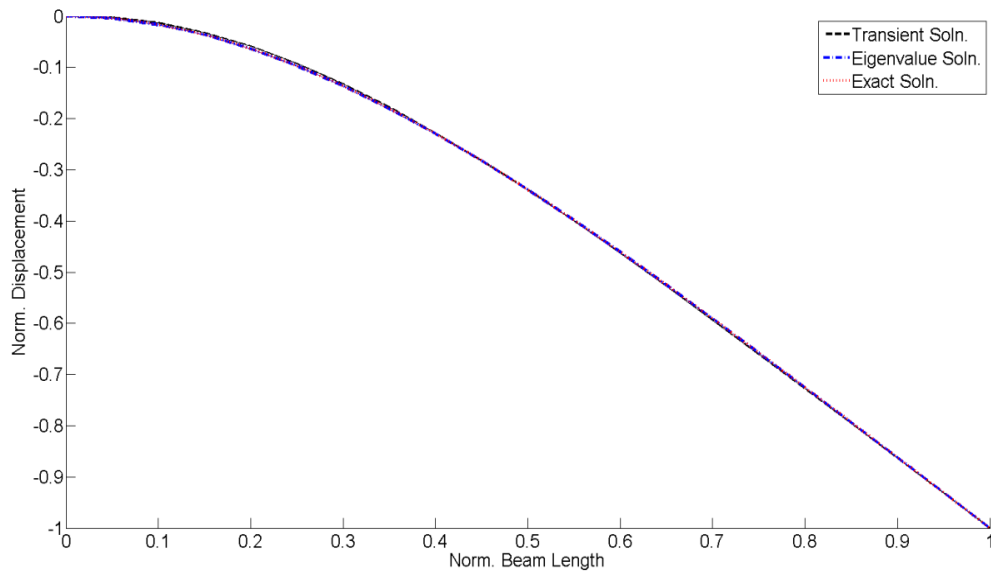


Figure 6. Cantilever Beam Using 20 Elements—Mode 1.

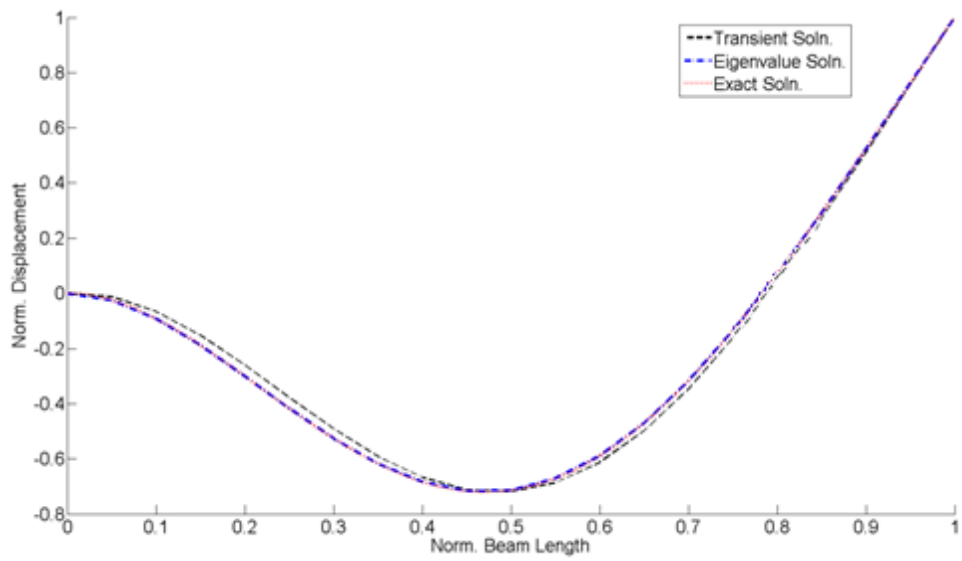


Figure 7. Cantilever Beam Using 20 Elements—Mode 2.

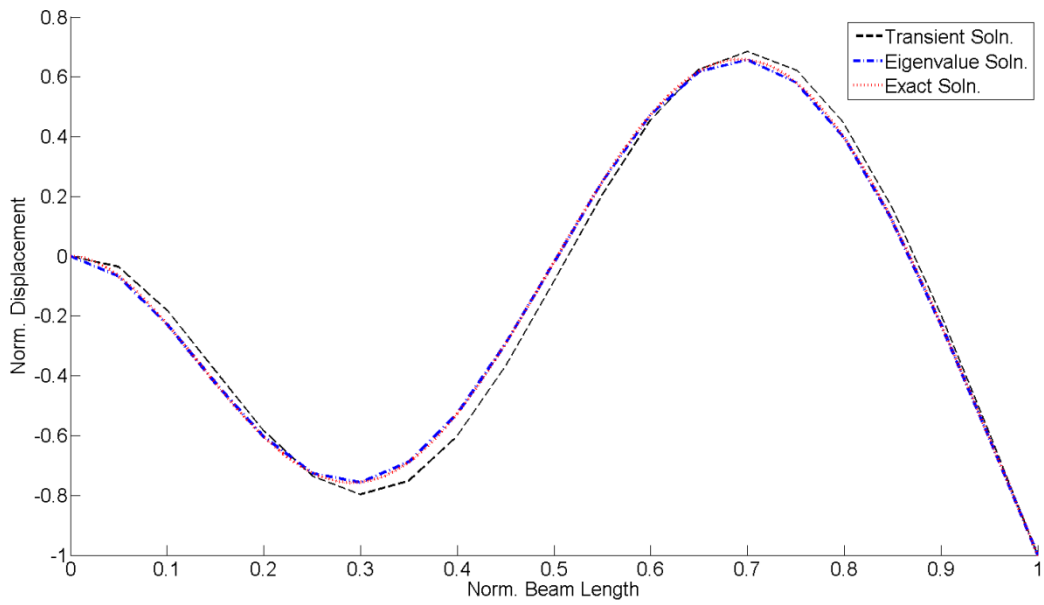


Figure 8. Cantilever Beam Using 20 Elements—Mode 3.

c. Comparison of Solutions for Cantilever Beam Using 40 Finite Elements

Figure 9. through Figure 11. compare the first three mode shapes of a cantilever beam using 40 elements. Table 3. compares the first five natural frequencies.

Cantilever 40 Elements	Natural Frequency Exact Solution	Natural Frequency Eigenvalues Solution	Natural Frequency Transient Solution
Mode 1	25.54	25.54 (0%)	26.20 (2.58 %)
Mode 2	160.06	160.06 (0%)	160.00 (0.03 %)
Mode 3	448.19	448.19 (0%)	460.00 (2.63 %)
Mode 4	878.27	878.28 (0.001 %)	890.00 (1.33 %)
Mode 5	1451.85	1451.87 (0.001 %)	1480.00 (1.93 %)

Table 3. Cantilever Beam Using 40 Elements—Natural Frequencies for the First Five Modes in Air.

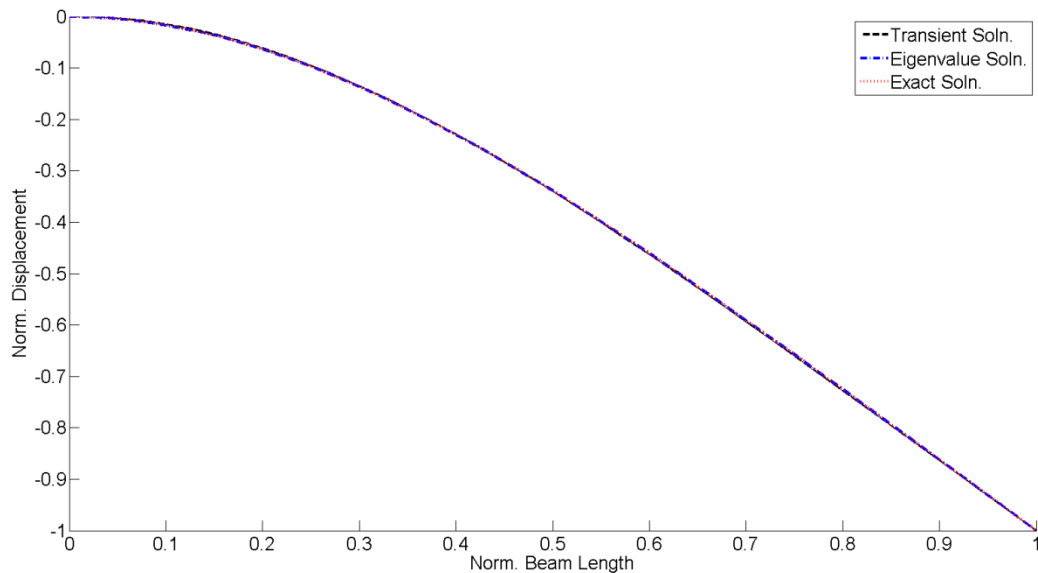


Figure 9. Cantilever Beam Using 40 Elements—Mode 1.

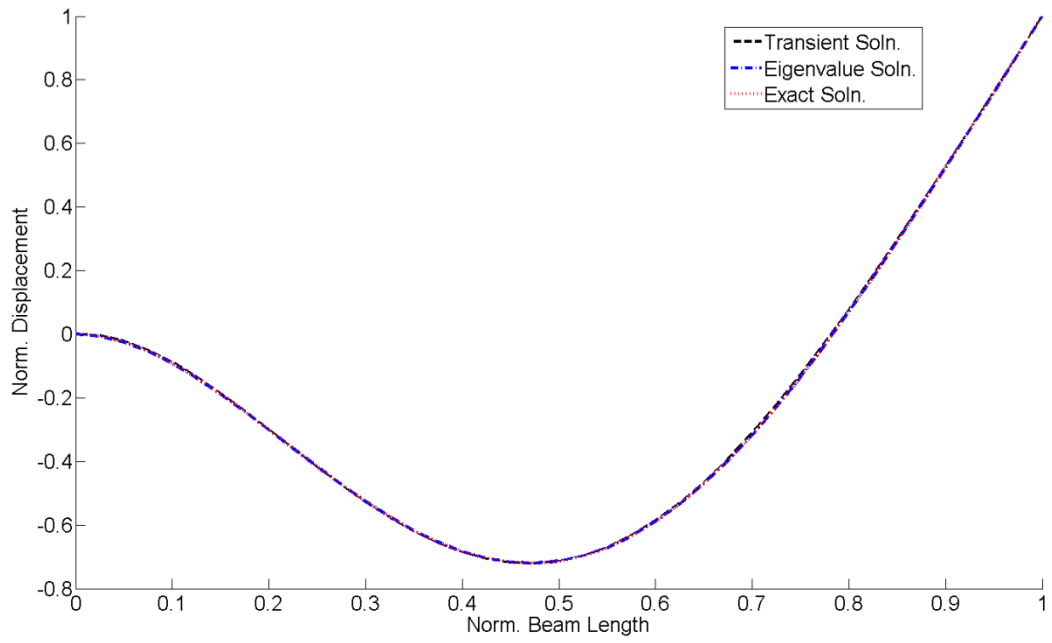


Figure 10. Cantilever Beam Using 40 Elements—Mode 2.

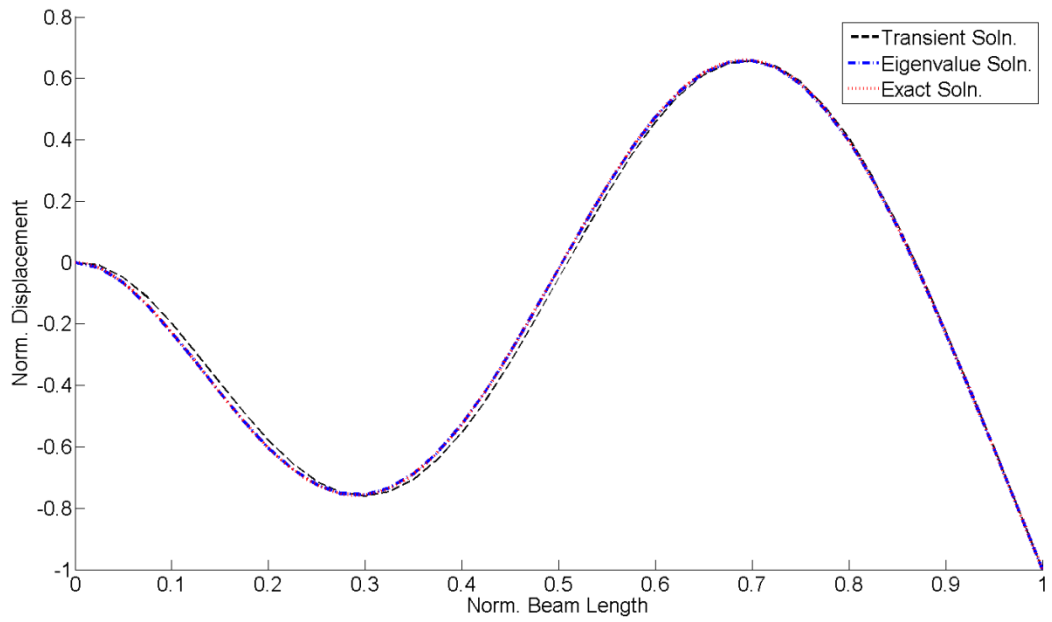


Figure 11. Cantilever Beam Using 40 Elements—Mode 3.

d. Comparison of Solutions for Pinned-Pinned Beam Using Ten Finite Elements

Figure 12. through Figure 14. compare the first three mode shapes of a simply supported beam using ten elements. Table 4. compares the first five natural frequencies.

Pinned-Pinned 10 Elements	Natural Frequency Exact Solution	Natural Frequency Eigenvalues Solution	Natural Frequency Transient Solution
Mode 1	71.69	71.69 (0 %)	73.00 (1.82 %)
Mode 2	286.78	286.81 (0.01 %)	308.00 (7.38 %)
Mode 3	645.27	645.61 (0.05 %)	690.00 (6.93 %)
Mode 4	1147.14	1149.04 (0.16 %)	1230.00 (7.22 %)
Mode 5	1792.41	1799.49 (0.39 %)	1930.00 (7.67 %)

Table 4. Pinned-Pinned Beam Using Ten Elements—Natural Frequencies for the First Five Modes in Air.

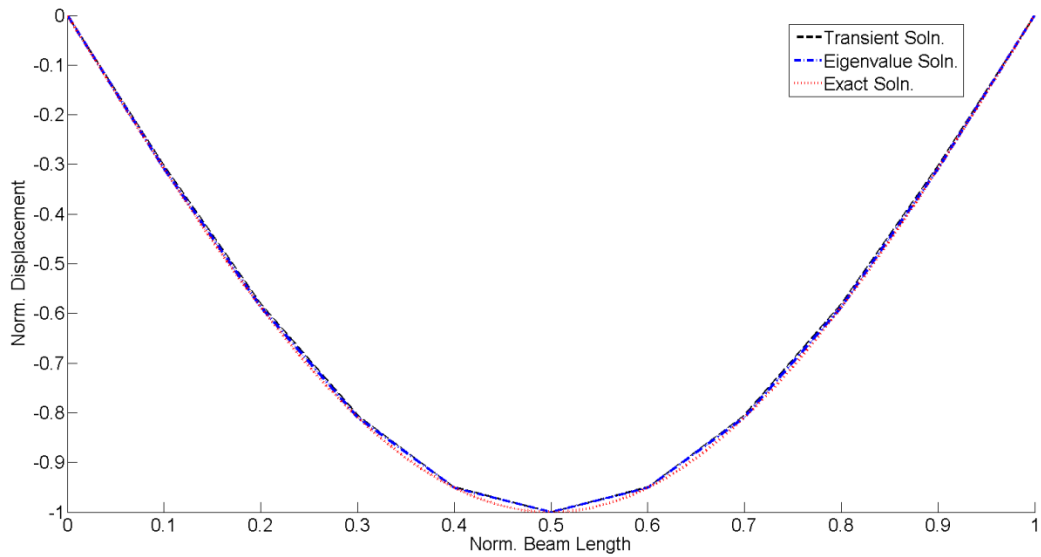


Figure 12. Pinned-Pinned Beam Using Ten Elements—Mode 1.

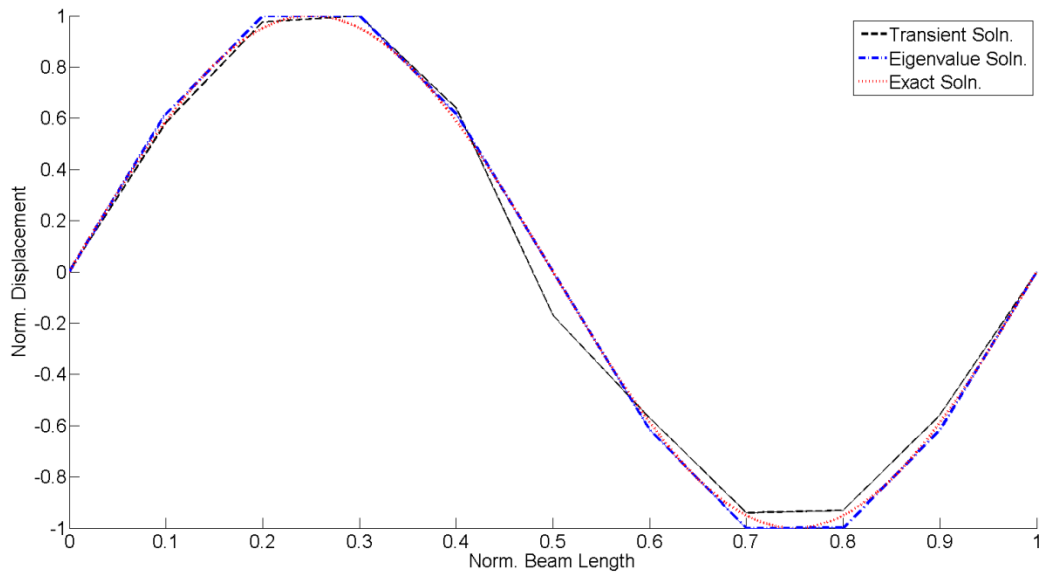


Figure 13. Pinned-Pinned Beam Using Ten Elements—Mode 2.

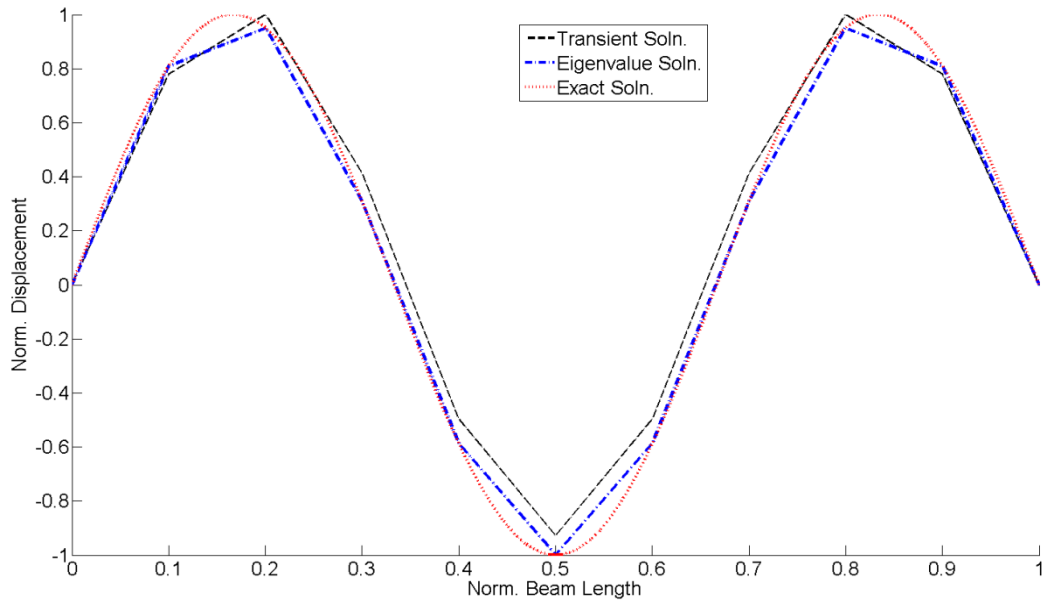


Figure 14. Pinned-Pinned Beam Using Ten Elements—Mode 3.

e. Comparison of Solutions for Pinned-Pinned Beam Using 20 Finite Elements

Figure 15. through Figure 17. compare the first three mode shapes of a simply supported beam using 20 elements. Table 5. compares the first five natural frequencies.

Pinned-Pinned 20 Elements	Natural Frequency Exact Solution	Natural Frequency Eigenvalues Solution	Natural Frequency Transient Solution
Mode 1	71.69	71.69 (0 %)	70.00 (2.35 %)
Mode 2	286.78	286.78 (0 %)	300.00 (4.60%)
Mode 3	645.27	645.29 (0.003 %)	670.00 (3.83 %)
Mode 4	1147.14	1147.27 (0.011 %)	1190.00 (3.73 %)
Mode 5	1792.41	1792.88 (0.026 %)	1850.00 (3.21 %)

Table 5. Pinned-Pinned Beam Using 20 Elements—Natural Frequencies for the First Five Modes in Air.

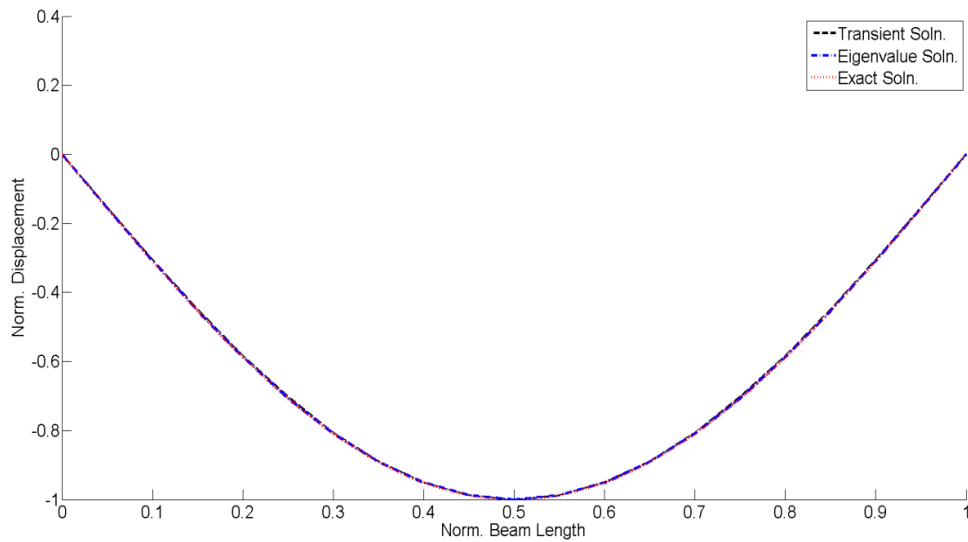


Figure 15. Pinned-Pinned Beam Using 20 Elements—Mode 1.

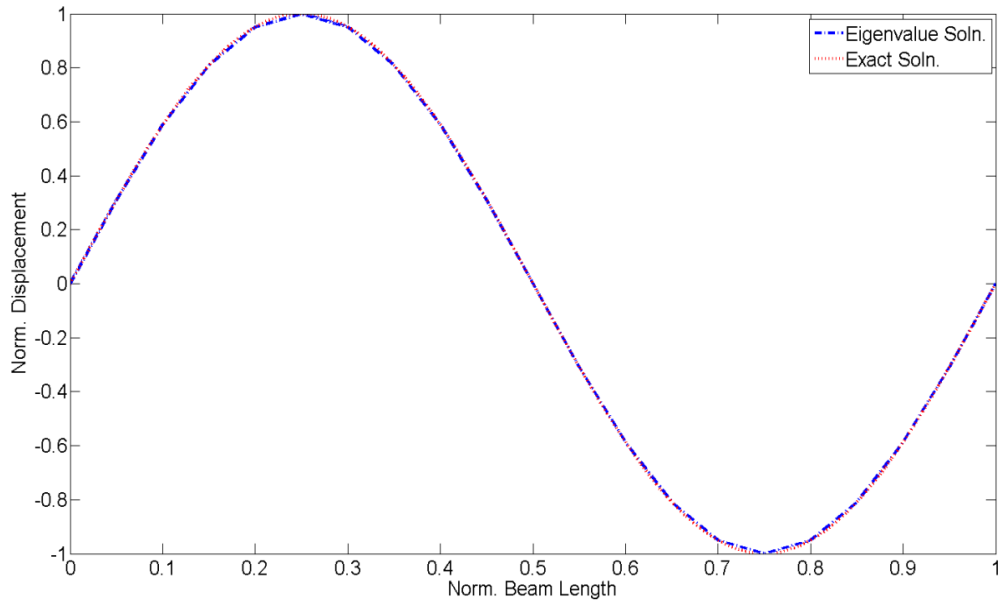


Figure 16. Pinned-Pinned Beam Using 20 Elements—Mode 2.

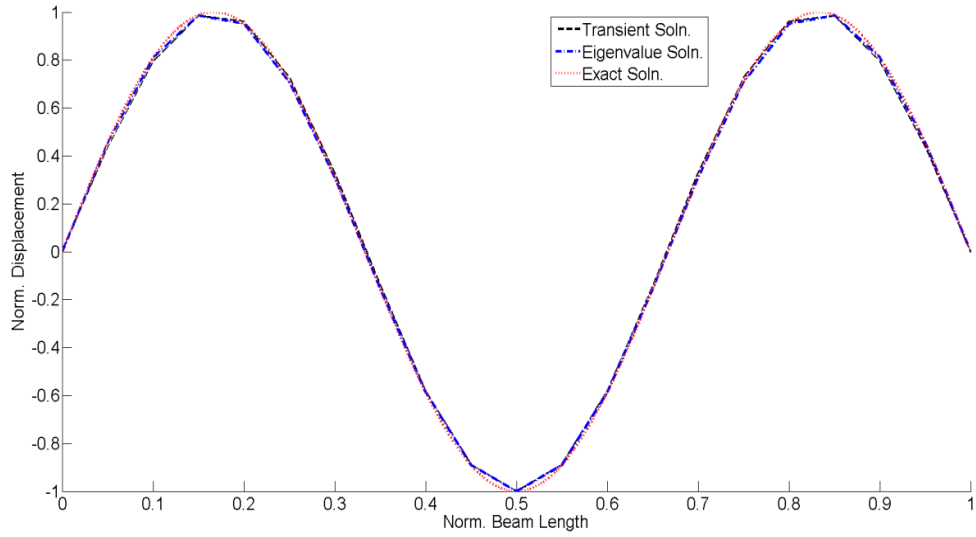


Figure 17. Pinned-Pinned Beam Using 20 Elements—Mode 3.

f. Comparison of Solutions for Pinned-Pinned Beam Using 40 Finite Elements

Figure 18. through Figure 20. compare the first three mode shapes of a simply supported beam using 40 elements. Table 6. compares the first five natural frequencies.

Pinned-Pinned 40 Elements	Natural Frequency Exact Solution	Natural Frequency Eigenvalues Solution	Natural Frequency Transient Solution
Mode 1	71.69	71.69 (0 %)	70.00 (2.35 %)
Mode 2	286.78	286.78 (0 %)	290.00 (1.12 %)
Mode 3	645.27	645.27 (0 %)	660.00 (2.28 %)
Mode 4	1147.14	1147.15 (0.0008 %)	1160.00 (1.12 %)
Mode 5	1792.41	1792.44 (0.001 %)	1820.00 (1.53 %)

Table 6. Pinned-Pinned Beam Using 40 Elements—Natural Frequencies for the First Five Modes in Air.

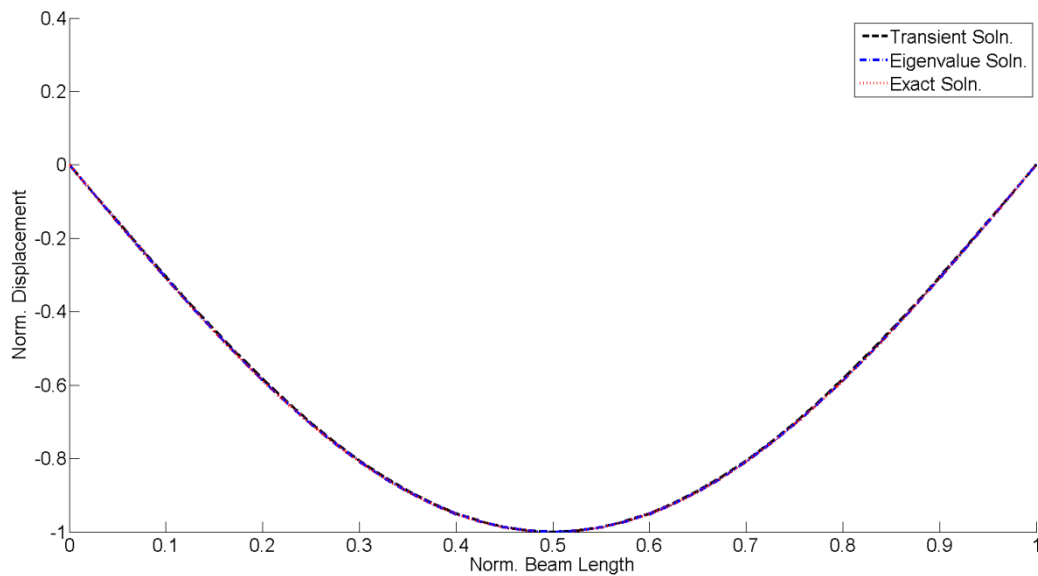


Figure 18. Pinned-Pinned Beam Using 40 Elements—Mode 1.

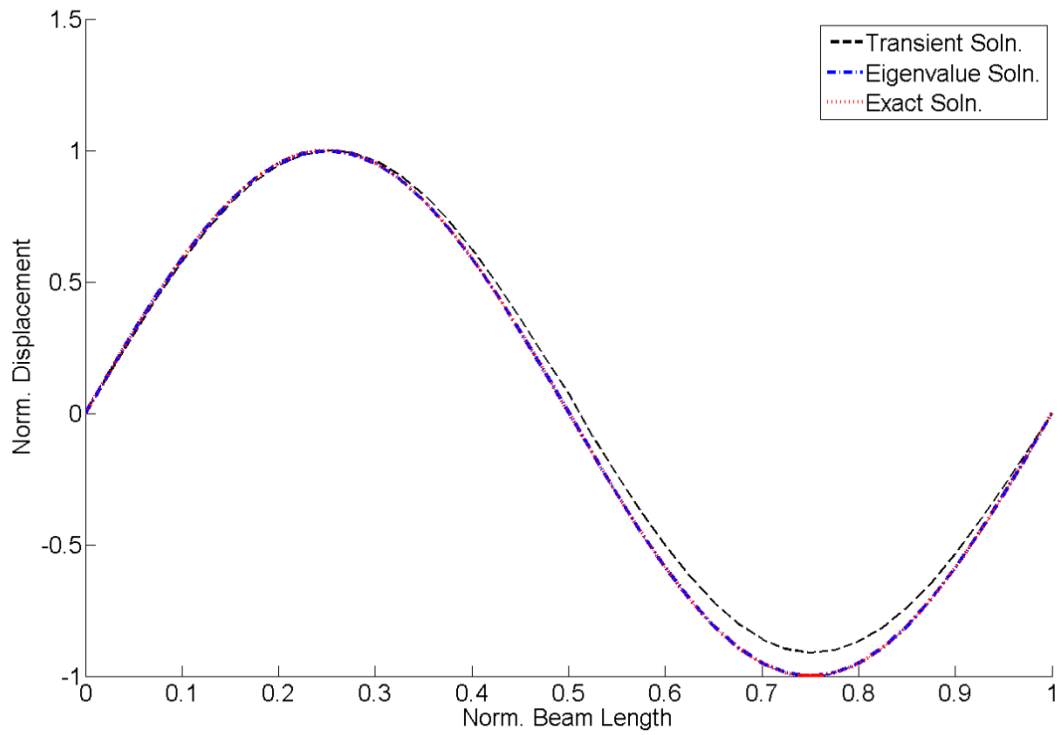


Figure 19. Pinned-Pinned Beam Using 40 Elements—Mode 2.

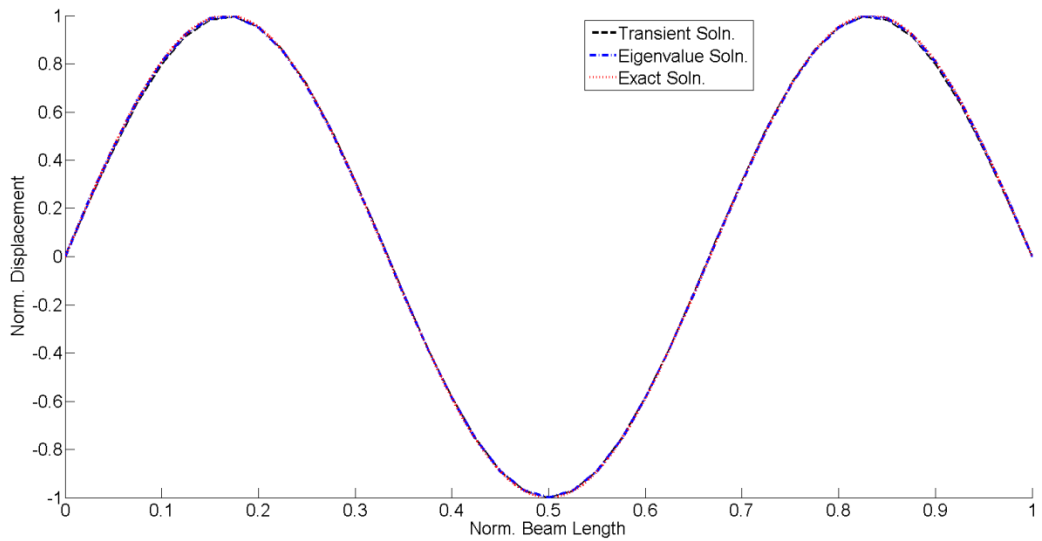


Figure 20. Pinned-Pinned Beam Using 40 Elements—Mode 3.

g. Comparison of Solutions for Clamped-Clamped Beam Using Ten Finite Elements

Figure 21. through Figure 23. compare the first three mode shapes of a clamped-clamped beam using ten elements. Table 7. compares the first five natural frequencies.

Clamped-Clamped 10 Elements	Natural Frequency Exact Solution	Natural Frequency Eigenvalues Solution	Natural Frequency Transient Solution
Mode 1	162.52	162.53 (0.0006 %)	178.39 (9.52 %)
Mode 2	448.01	448.13 (0.026 %)	493.12 (10.04 %)
Mode 3	878.29	879.15 (0.015 %)	994.32 (13.08 %)
Mode 4	1500.41	1455.69 (2.9 %)	1680.00 (11.96 %)
Mode 5	2168.82	2181.23 (0.57 %)	2520.00 (16.19 %)

Table 7. Clamped-Clamped Beam Using 10 Elements—Natural Frequencies for the First Five Modes in Air.

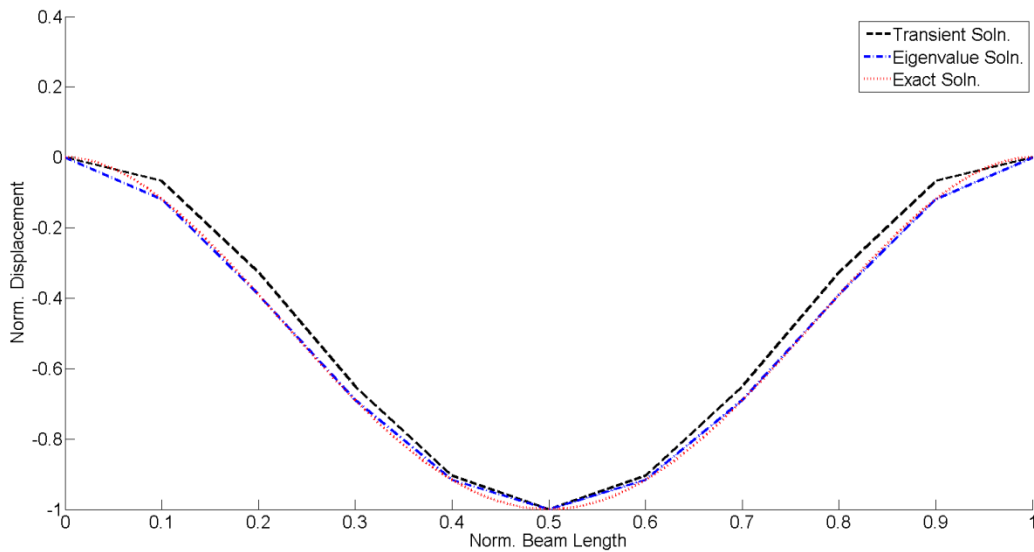


Figure 21. Clamped-Clamped Beam Using Ten Elements—Mode 1.

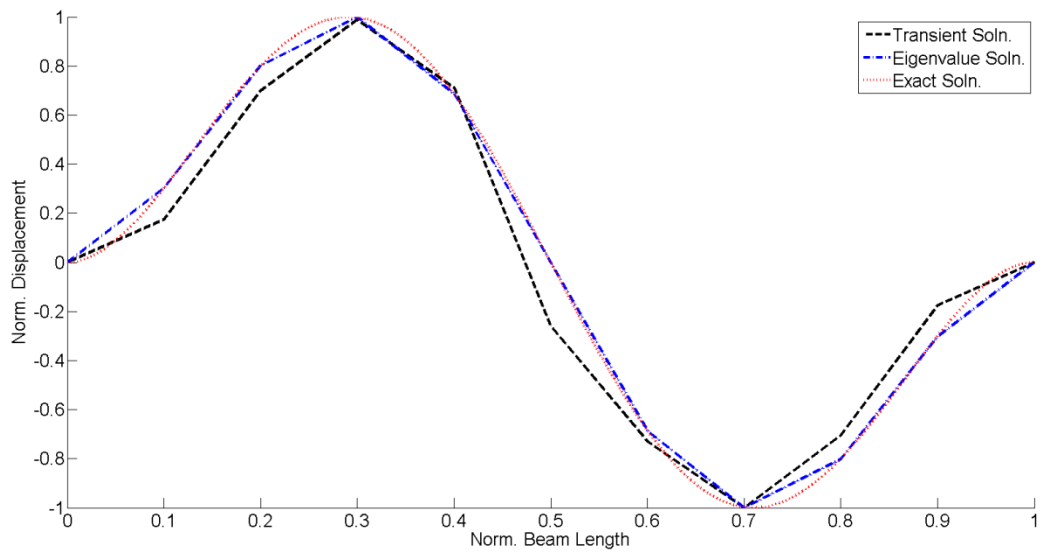


Figure 22. Clamped-Clamped Beam Using Ten Elements—Mode 2.

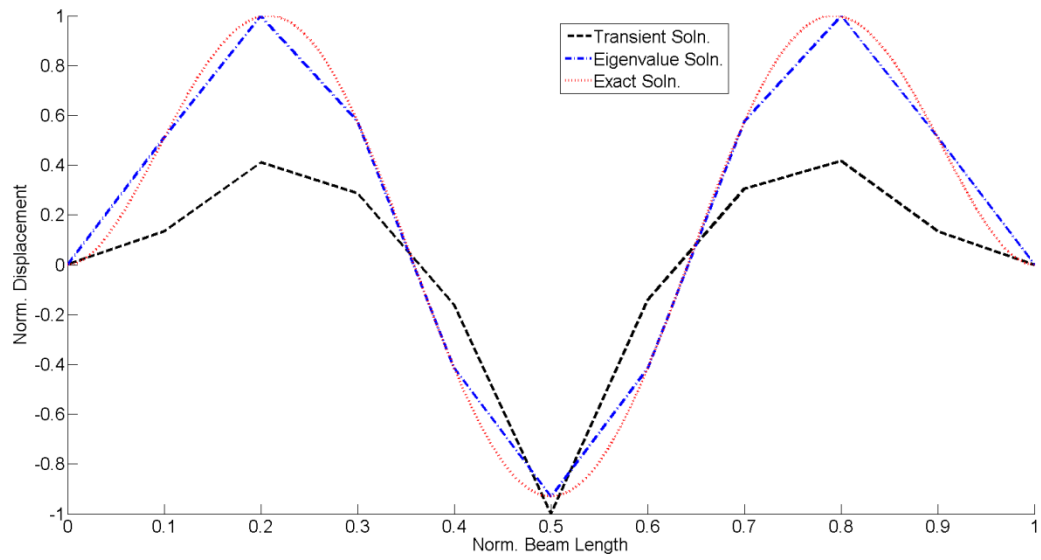


Figure 23. Clamped-Clamped Beam Using Ten Elements—Mode 3.

h. Comparison of Solutions for Clamped-Clamped Beam Using 20 Finite Elements.

Figure 24. through Figure 26. compare the first three mode shapes of a clamped-clamped beam using 20 elements. Table 8. compares the first five natural frequencies.

Clamped-Clamped 20 Elements	Natural Frequency Exact Solution	Natural Frequency Eigenvalues Solution	Natural Frequency Transient Solution
Mode 1	162.52	162.52 (0 %)	170.00 (4.6 %)
Mode 2	448.01	448.02 (0.002 %)	480.00 (7.14 %)
Mode 3	878.29	878.34 (0.005 %)	940.00 (7.02 %)
Mode 4	1500.41	1452.10 (3.21 %)	1560.00 (3.97 %)
Mode 5	2168.82	2169.64 (0.037 %)	2320.00 (6.97 %)

Table 8. Clamped-Clamped Beam Using 20 Elements—Natural Frequencies for the First Five Modes in Air.

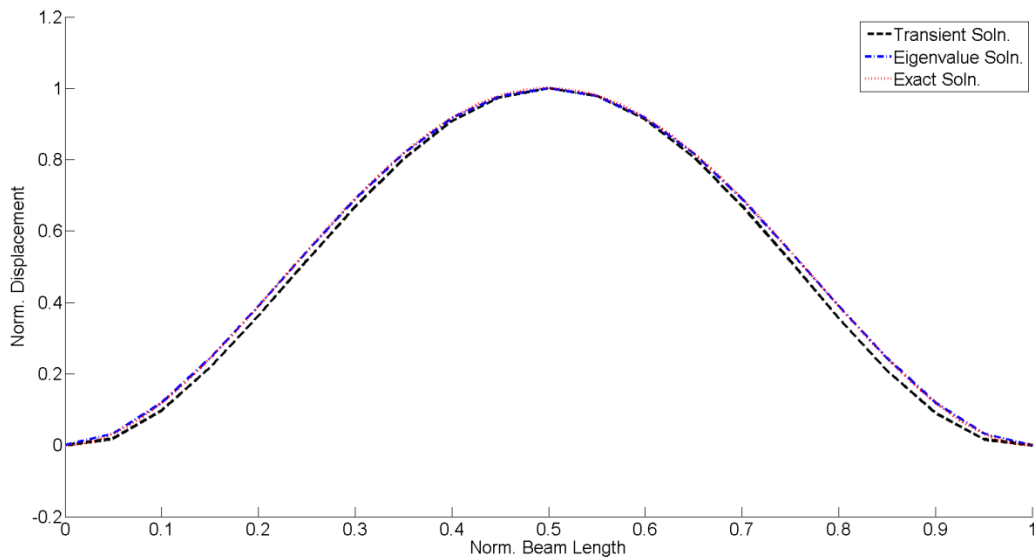


Figure 24. Clamped-Clamped Beam Using 20 Elements—Mode 1.

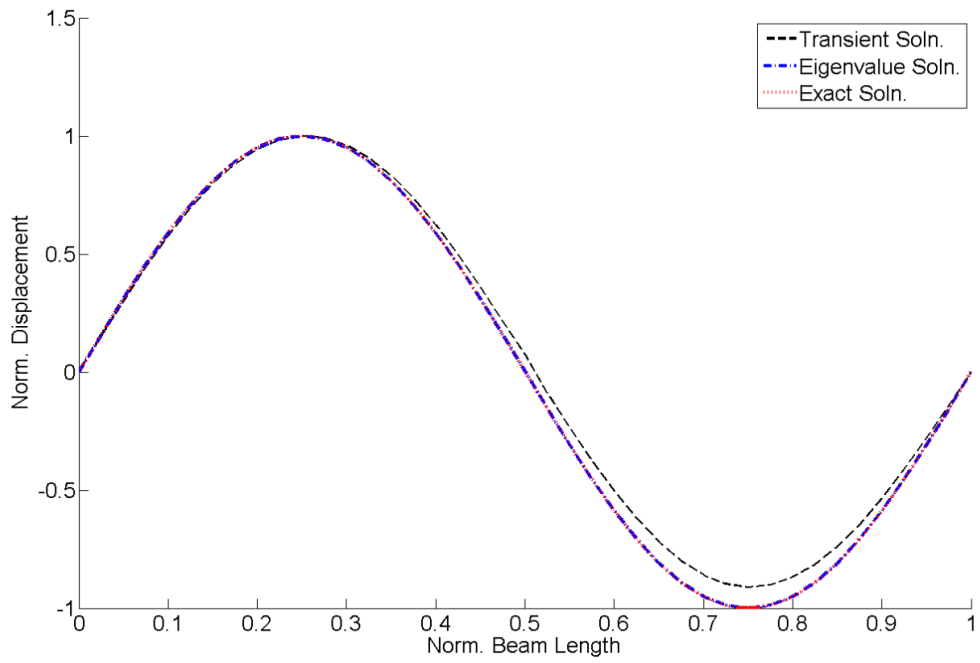


Figure 25. Clamped-Clamped Beam Using 20 Elements—Mode 2.

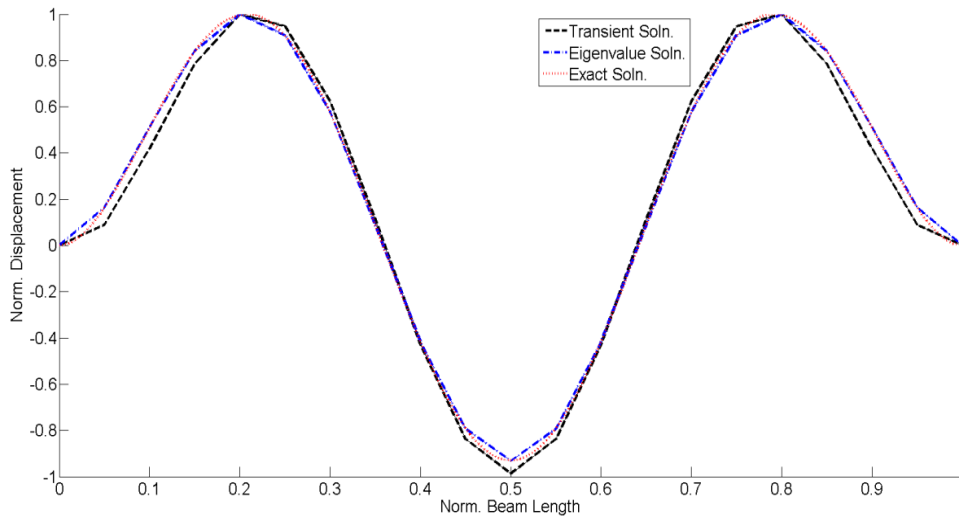


Figure 26. Clamped-Clamped Beam Using 20 Elements—Mode 3.

i. Comparison of Solutions for Clamped-Clamped Beam Using 40 Finite Elements.

Figure 27. through Figure 29. compare the first three mode shapes of a clamped-clamped beam using 40 elements. Table 9. compares the first five natural frequencies.

Clamped-Clamped 40 Elements	Natural Frequency Exact Solution	Natural Frequency Eigenvalues Solution	Natural Frequency Transient Solution
Mode 1	162.52	162.52 (0 %)	170.00 (4.6 %)
Mode 2	448.01	448.01 (0 %)	460.00 (2.67 %)
Mode 3	878.29	878.29 (0 %)	910.00 (3.61 %)
Mode 4	1500.41	1451.87 (3.23 %)	1500.00 (0.027 %)
Mode 5	2168.82	2168.87 (0.002%)	2240.00 (3.28 %)

Table 9. Clamped-Clamped Beam Using 40 Elements—Natural Frequencies for the First Five Modes in Air.

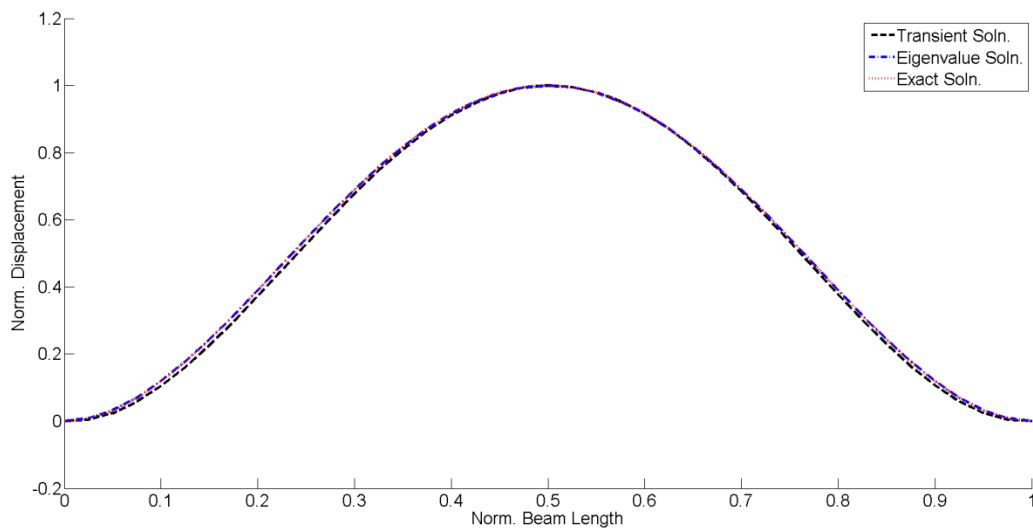


Figure 27. Clamped-Clamped Beam Using 40 Elements—Mode 1.

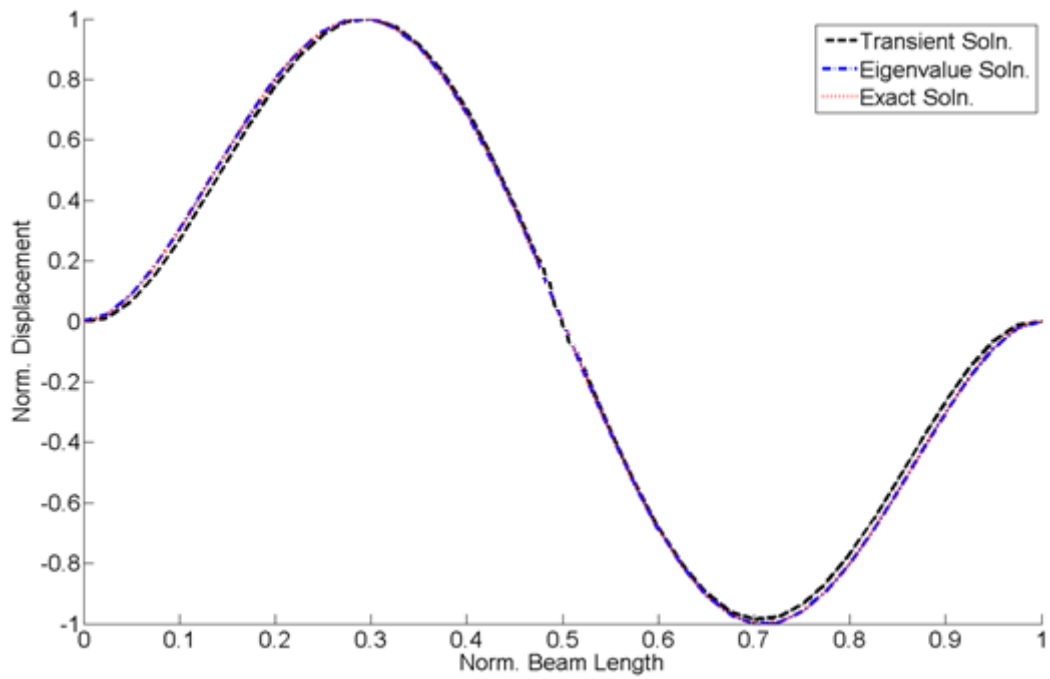


Figure 28. Clamped-Clamped Beam Using 40 Elements—Mode 2.

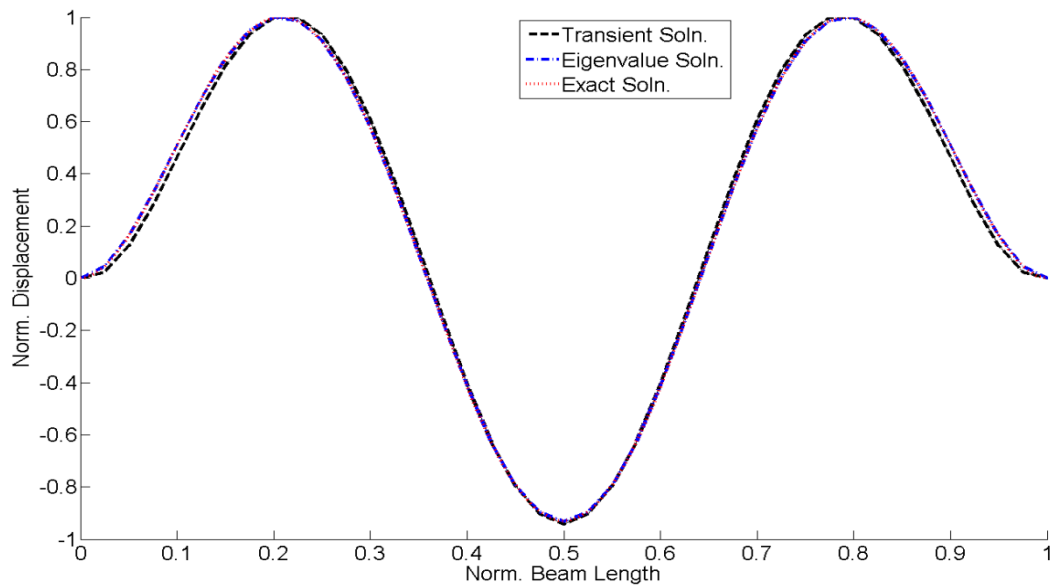


Figure 29. Clamped-Clamped Beam Using 40 Elements—Mode 3.

B. SUMMARY OF COMPOSITE BEAM FINITE ELEMENT MODEL

The plots shown previously prove that our 2D-beam finite element model behaves in realistic way. That means that the model is providing a response that is almost equal to or a very close approximation of the expected response. For example, the mode shapes that are calculated from our FEM are close to the analytical mode shapes of the beam. When the number of finite elements is large and the number of time steps big ‘enough’ then the mode shapes are almost identical to the analytical solution of the mode shapes. The three different solutions—the transient, the eigenvalue, and the analytical solutions—agree with one another.

We observe that even using only ten finite elements the program provides very accurate results for the first mode. But in order to more accurately ‘capture’ and represent the behavior of the beam in higher modes, more finite elements need to be used for the analysis. That is well known and expected, because in order to capture larger changes in deflections and slopes, we need to imply higher ‘resolution’ of the model. We need to make the discretized pieces—i.e., finite elements—of the beam smaller so the mathematical solution that the program provides would be closer to the actual ‘real-world,’ where, of course, the beam is continuous.

The effect of the fluid-structure interaction on the dynamic response of the beam has proved to be significant. For the FSI case, the vibrational energy is getting ‘stored’ into the higher modes. That means that higher frequencies are excited because of the interaction with the fluid. The FSI alters the response of the structure, changes the mode shapes, and mostly affects the beam’s behavior in higher vibration modes [4].

Since the modal curvatures at the beam modes are directly related to the bending strain of the beam, we see that the FSI effect has an impact on the structural integrity of the beam. There are large difference in the nodal displacement and curvature between the FSI and the non-FSI case.

IV. COMPOSITE BEAM FEM INCLUDING FLUID-STRUCTURE INTERACTION

The MATLAB program that we developed uses three interconnected/coupled models for the calculations. One model is used for the generic fluid domain using the cellular automata (CA) method. The second model is a finite element model of those regions of the fluid that are adjacent to the beam. Finally, the third model is a finite element model used to represent the composite beam structure.

The CA and FEM models calculate the solutions independently, but they are coupled, meaning that the solution of each one is ‘passed’ to the input of the other [5]. Because the solution we seek is the transient not the steady-state solution, the whole set of calculations is done with a time-marching technique. That means that all calculations are made for each time step. Then the set of solutions for each time step is ‘fed’ as input to the next time step. After enough time steps, the solution is complete.

The transient dynamic response (i.e., the deflections, the slopes, the curvatures, the mode shapes, and the natural frequencies) were calculated by running the MATLAB program that we developed. The natural frequencies have been ‘extracted’ using FFT. This allows us to evaluate which frequencies and corresponding modes are excited the most. In other words, it gives us an insight as to in which vibration modes there is more energy ‘stored.’ This is specifically critical in the case where fluid-structure interaction is included in the calculation, as it shows explicitly the behavior of the structure when it is submerged in water.

The data used in the models were the following:

- The beam material is composite material.
- Young’s modulus of elasticity $E=20\text{GPa}$.
- Poisson’s ratio $\nu=0.3$.
- Beam density $\rho=2000\text{ kgr/m}^3$.
- Beam’s length=1m.
- Beam’s width=0.1m.
- Beam’s depth (or thickness)=0.05m.

- The fluid is assumed to be water. It is assumed that there is no fluid flow and no viscosity in the fluid medium.
- Water density=1,000 kg/m³.
- Speed of sound in the fluid medium is $c=1,500$ m/sec.
- The boundary conditions of the beam are clamped at both ends.

A. COMPOSITE BEAM FEM CALCULATIONS

The FFT was used as a tool to ‘extract’ the natural frequencies from the computational experiments that had been done using the FEM program. By observing the natural frequencies that ‘live’ on x-axis we interpreted and understood the regions of the beam’s natural frequencies spectrum which were excited the most. Just like the actual experimental sample, we treated the solutions of the FEM program, such as the nodal displacements of the beam, as being data from a physical experimental analysis. Then we applied the MATLAB embedded function ‘fft’ on each displacement degree of freedom. The resulting plots of the first three mode shapes for each of the aforementioned cases are provided.

1. Clamped-Clamped Beam—No Fluid-Structure Interaction

The resulting plots as seen in Figure 30. and Figure 31. show the mode shapes that were calculated from our finite element program for the case where no fluid-structure interaction was included, assuming the beam was surrounded by air, the initial displacement of the beam was zero, and an impulse load was applied on the displacement dof of the center of the beam.

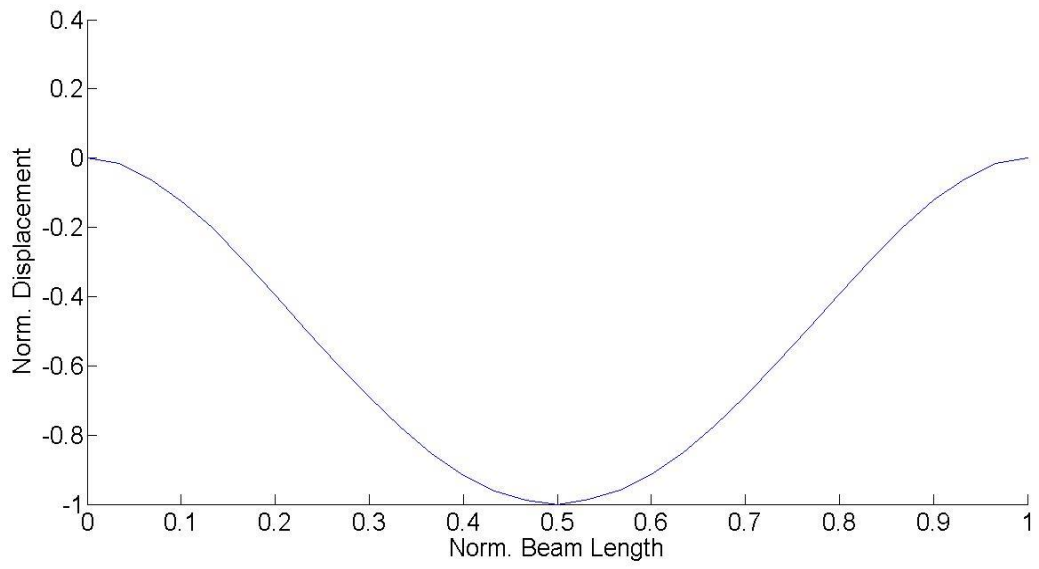


Figure 30. Clamped-Clamped Beam–Mode 1 without FSI.

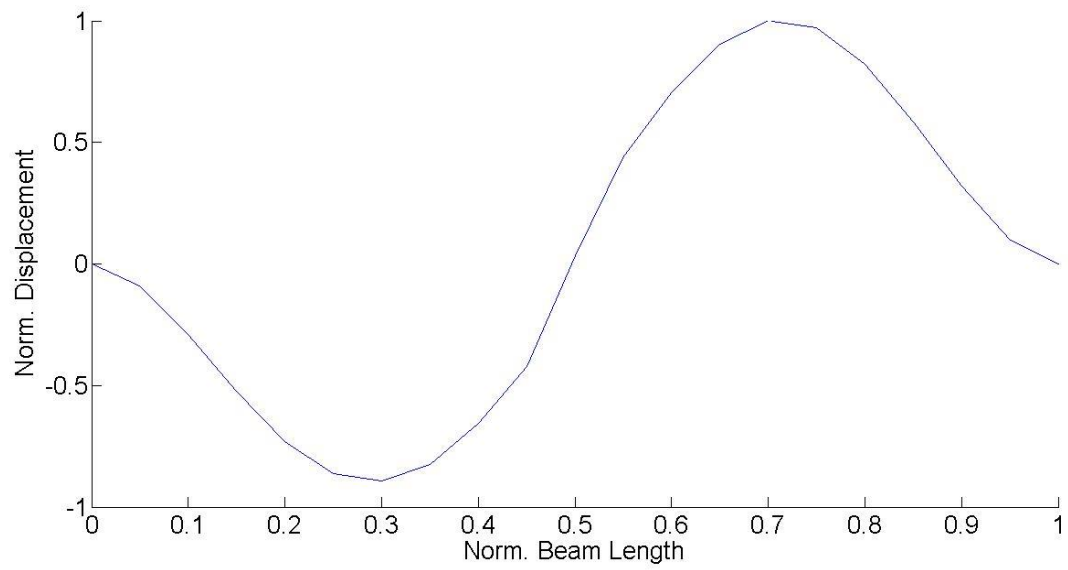


Figure 31. Clamped-Clamped Beam–Mode 2 without FSI.

2. Clamped-Clamped Beam—Fluid-Structure Interaction Included

The following plots in Figure 32. and Figure 33. were calculated from the program for the case where fluid-structure interaction was included. It assumes the beam is surrounded by water. The mode shapes are plotted against those mode shapes calculated without the FSI effects for comparison and validation purposes. These calculations do not include any applied load.

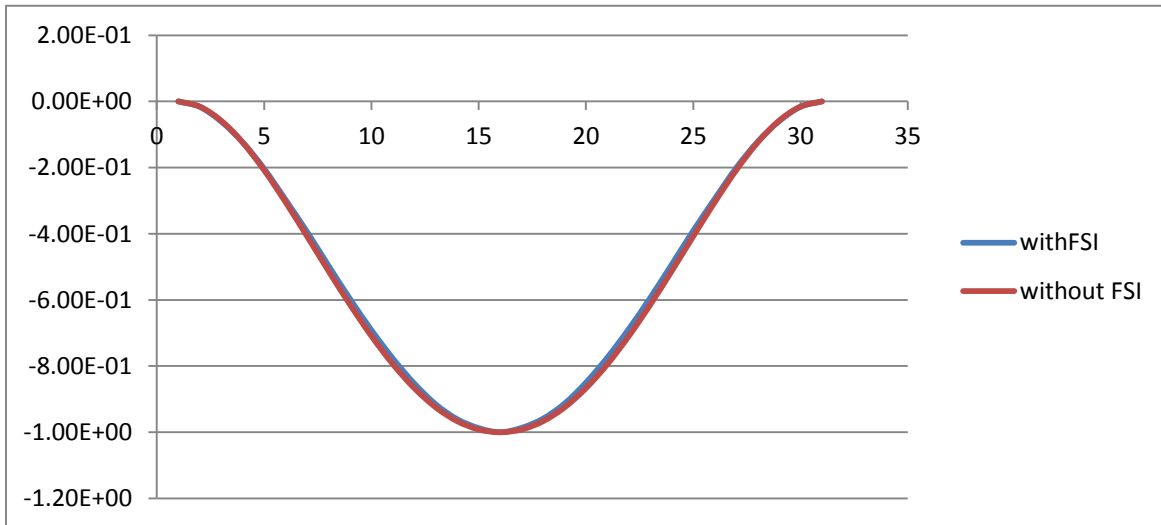


Figure 32. Clamped-Clamped Beam—Mode 1 with FSI.

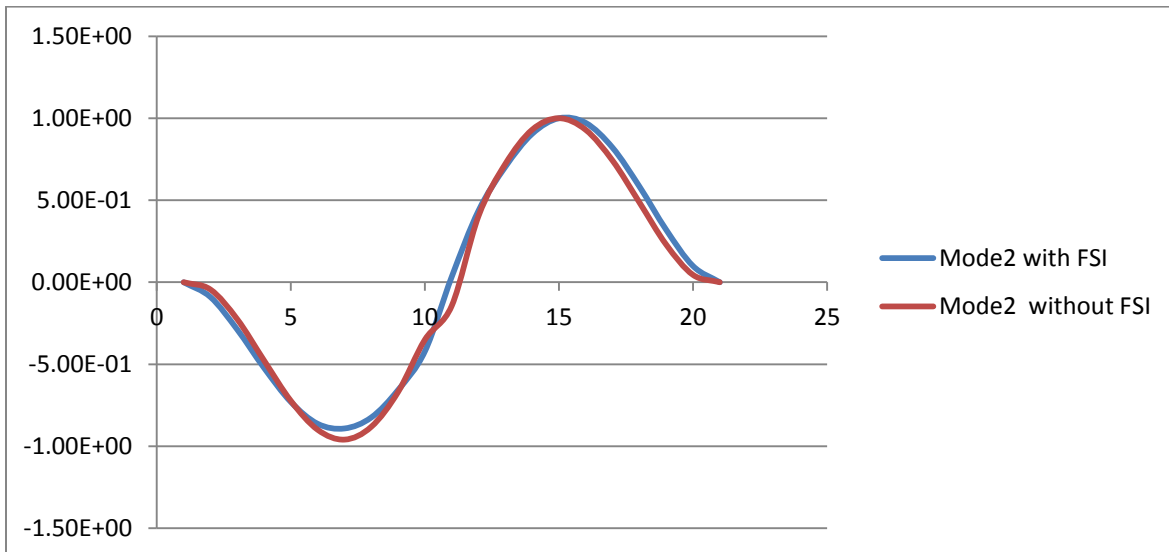


Figure 33. Clamped-Clamped Beam—Mode 2 with FSI.

3. Natural Frequencies—No Fluid-Structure Interaction

Table 10. shows the natural frequencies of the first three modes of the beam and the associated error—compared to the exact/analytical solution—that were calculated from the program for the case where no fluid-structure interaction was included and assuming the beam was surrounded by air. The initial condition of this simulation was that the beam had zero displacement. There was no load applied on the beam. All frequencies are in Hz.

	Natural Frequency Exact Solution	Natural Frequency Eigenvalues Solution	Natural Frequency Transient Solution
Mode 1	162.52	162.52 (0 %)	169.70 (4.41 %)
Mode 2	448.01	448.01 (0 %)	424.30 (5.29 %)
Mode 3	878.29	878.29 (0 %)	827.30 (3.61 %)

Table 10. Natural Frequencies without FSI.

4. Natural Frequencies—Fluid-Structure Interaction Included

Table 11. shows the natural frequency of the first mode of the beam that was calculated from the program for the case where fluid-structure interaction was included and assuming the beam was surrounded by water. The initial condition was that the beam had zero displacement. An impulse load was applied for this case. The natural frequencies values for the No FSI case are presented for the purpose of comparison and validation. All frequencies are in Hz.

	Natural Frequency Transient Solution Without FSI	Natural Frequency Transient Solution With FSI
Mode 1	169.70	63.64

Table 11. Comparison of Natural Frequency with and without FSI for Impulse Load.

B. COMPOSITE BEAM FSI FFT RESULTS FOR DIFFERENT LOADS OR INITIAL CONDITIONS

In the next case, the 2D composite beam was tested using our finite element program, setting different initial conditions and loads. The beam was computationally-virtually ‘held’ in zero displacement, which was the initial conditions, and then an impulse forcing load was applied on the displacement dof of a nodal location. We chose the location of the applied forcing load such that we could observe the vibration of the beam at every nodal point, avoiding any nodes (i.e., part of the beam that is not moving due to vibration modes cancelling each other out) that would show zero deflection. Next, we computationally applied the analytical statics solution for the deflection of the beam as initial conditions, and then we simulated two cases, one with an impulse forcing load and another without any applied load. The rest of the simulations were set up as the initial conditions being the analytical solution for mode shape one, two, and three. Again, one case included an impulse forcing load, while the other case did not include any load. After setting up the initial conditions as stated previously, the clamped-clamped beam was computationally ‘released’ to vibrate.

The FEM program, configured as previously mentioned, ran first with non-FSI and then with FSI included in the calculations. The solutions for the natural frequencies and the mode shapes were calculated first without fluid-structure interaction case and then with fluid-structure interaction included. Then they were plotted for comparison reasons.

The FFT technique applied on the nodal displacements provided us with a clear picture of the ‘distribution’ of the energy into the vibration modes, similarly to the FFT procedure that is used for the experimental data.

1. Statics Solution as Initial Conditions without Load—With and Without FSI

Figure 34. and Figure 35. are the frequency spectra of a clamped-clamped beam with and without FSI, respectively, when the beam had the Statics deflection as the initial condition which was obtained by applying a force at the center of the beam. No external load was applied during the simulation.

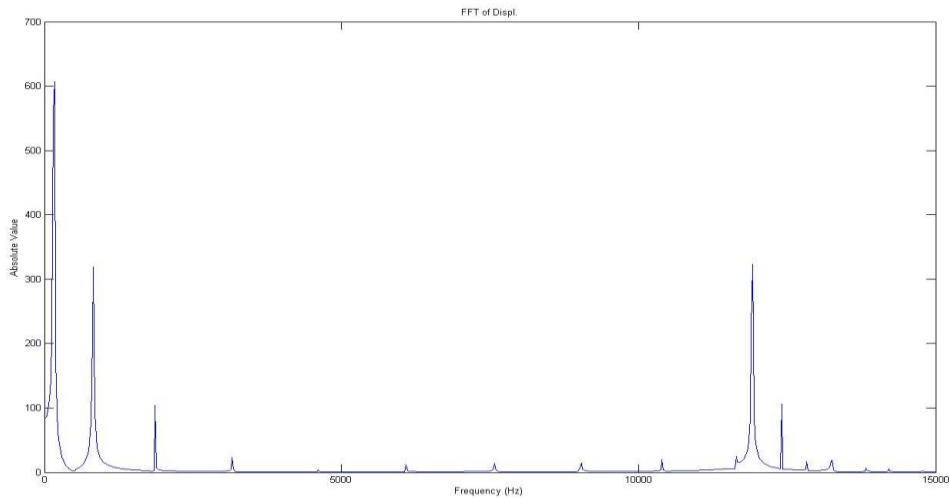


Figure 34. FFT of Displacement, without FSI.

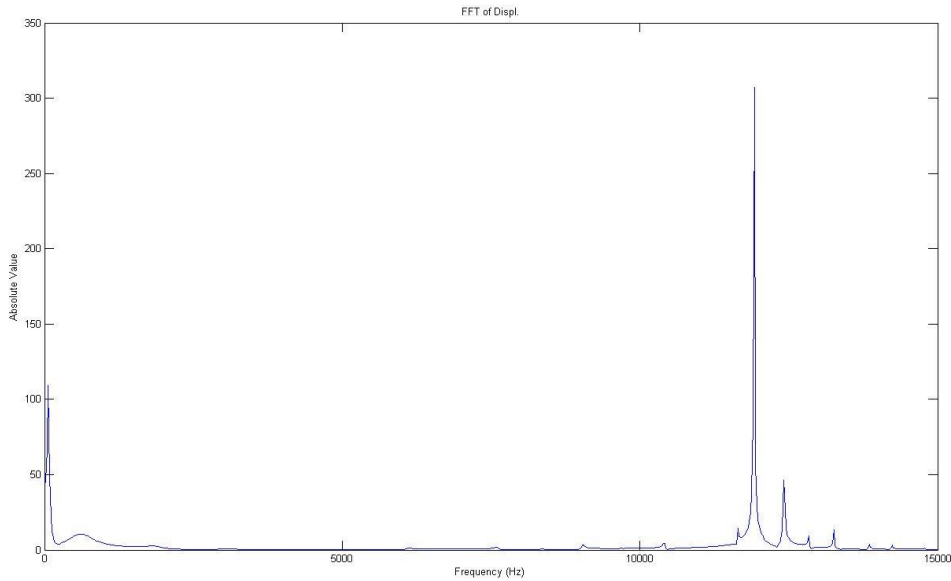


Figure 35. FFT of Displacement, with FSI.

Table 12. shows the natural frequency of the first mode of the beam that was calculated from the program for the case where fluid-structure interaction was included and assuming the beam was surrounded by water. The initial condition was that the beam had Statics displacement which was obtained by applying a force at the center of the beam. No load was applied for this case during the simulation. The natural frequencies values for the No FSI case are presented for the purpose of comparison and validation. All frequencies are in Hz.

	Natural Frequency Transient Solution Without FSI	Natural Frequency Transient Solution With FSI
Mode 1	169.70	63.64

Table 12. Comparison of Natural Frequency with and without FSI for Static Initial Displacement.

**2. Statics Solution as Initial Conditions with Impulse Forcing Load—
With and Without FSI**

Table 13. shows the natural frequency of the beam that was calculated from the program for the case where fluid-structure interaction was included and the fluid was water. The initial condition was that the beam had the Statics displacement which was obtained by applying a force at the center of the beam. In this case an impulse forcing load was applied during the simulation. All frequencies are in Hz.

	Natural Frequency Transient Solution Without FSI	Natural Frequency Transient Solution With FSI
Mode 1	169.70	63.64

Table 13. Comparison of Natural Frequency with and without FSI for Impulse Load and Statics Displacement.

**3. Zero Displacement as Initial Conditions with Impulse Forcing Load—
With and Without FSI**

Figure 36. and Figure 37. are the frequency spectra of a clamped-clamped beam with and without FSI, respectively, when the beam had the zero initial condition with an impulse load.

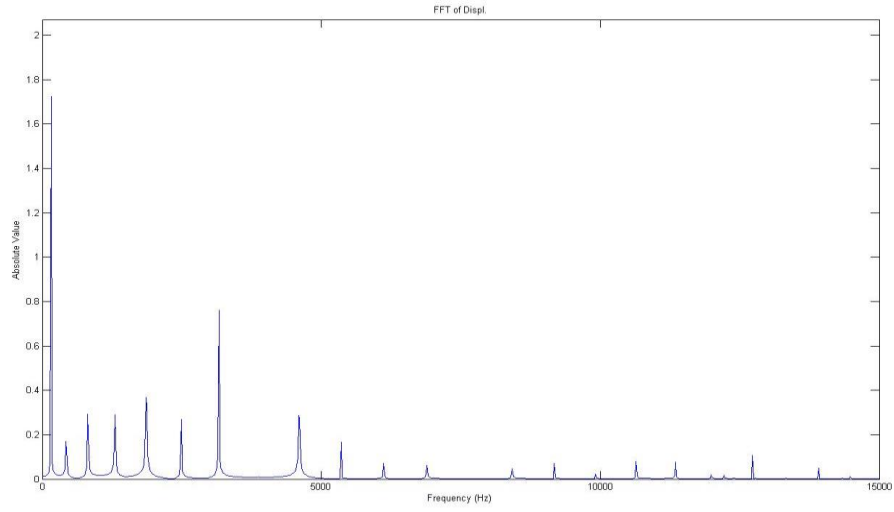


Figure 36. FFT of Displacement, without FSI.

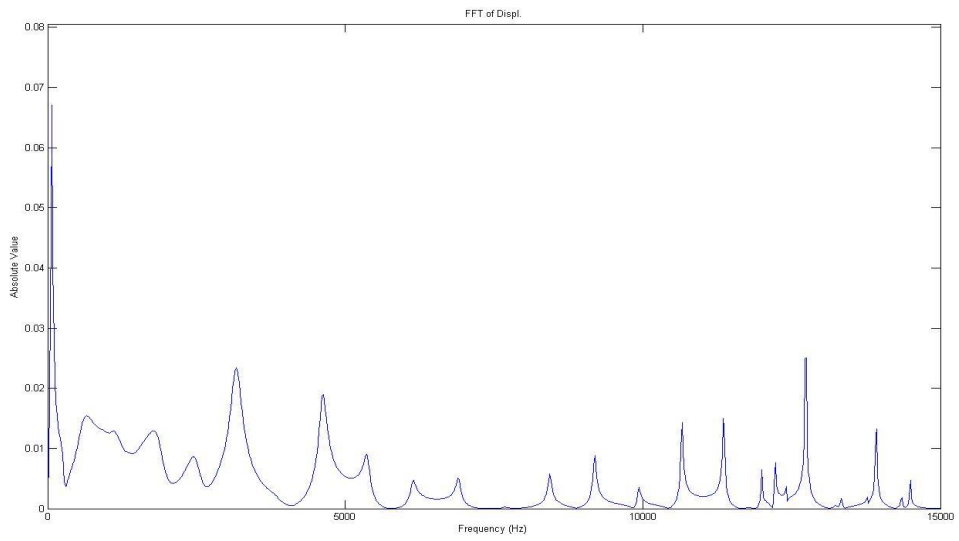


Figure 37. FFT of Displacement, with FSI.

Table 11. shows the natural frequency of the first mode of the beam that was calculated from the FEM program for this case. All frequencies are in Hz.

4. Mode 1 Displacement as Initial Conditions without Load—With and Without FSI

Figure 38. and Figure 39. are the frequency spectra of a clamped-clamped beam with and without FSI, respectively, when the beam had the first mode shape as the initial condition without any external load.

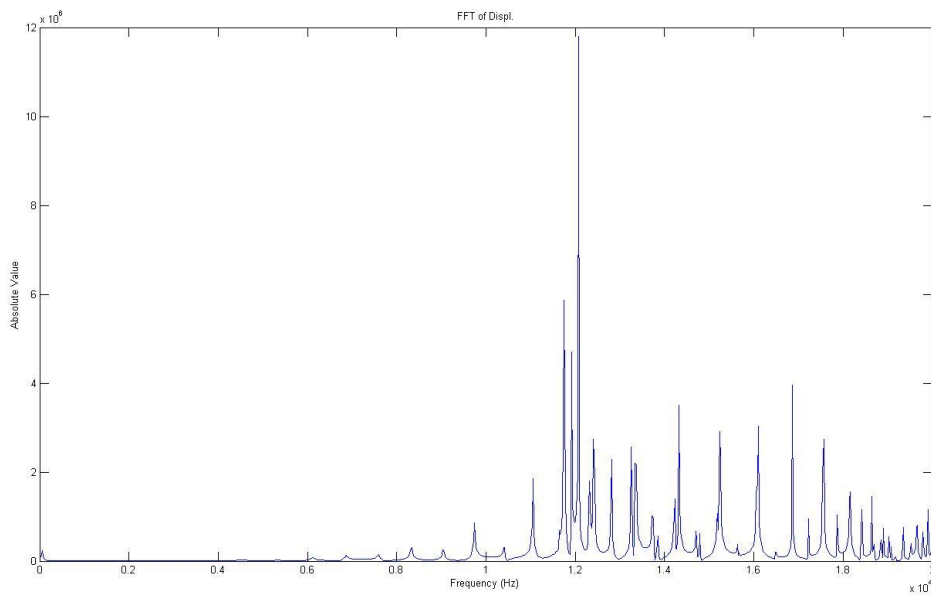


Figure 38. FFT of Displacement, without FSI.

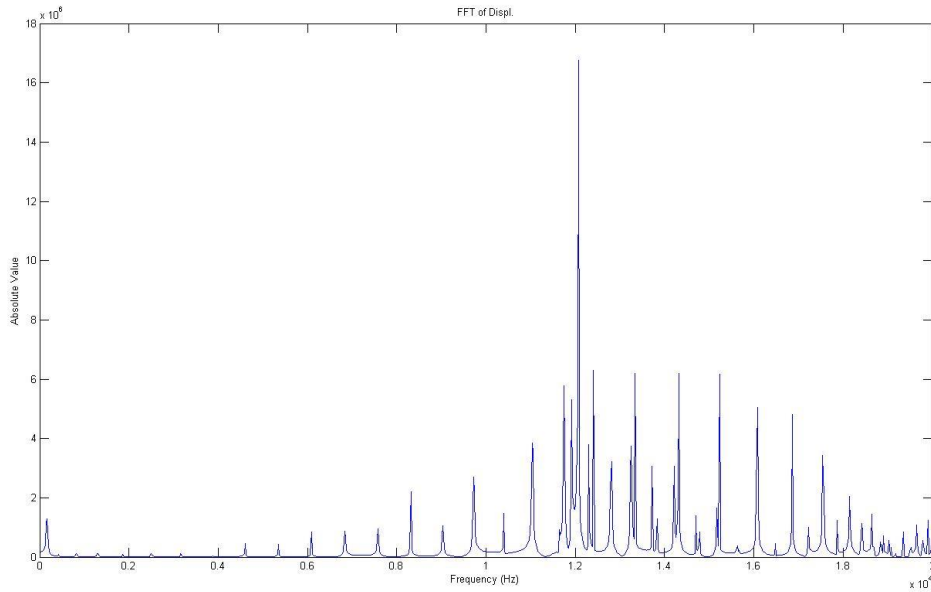


Figure 39. FFT of Displacement, with FSI.

Table 14. shows the natural frequency of the first mode of the beam for this case. All frequencies are in Hz.

	Natural Frequency Transient Solution Without FSI	Natural Frequency Transient Solution With FSI
Mode 1	169.70	63.64

Table 14. Comparison of Natural Frequency with and without FSI for Mode 1 Initial Displacement.

5. Mode 1 Displacement as Initial Conditions with Impulse Forcing Load—With and Without FSI

Table 15. shows the natural frequency of the first mode of the beam that was calculated from the program for the case where fluid-structure interaction was included and the fluid was water. The initial condition was that the beam had as initial displacement the analytical solution for the deflection of mode shape 1. In this case an impulse forcing load was applied during the simulation. All frequencies are in Hz.

	Natural Frequency Transient Solution Without FSI	Natural Frequency Transient Solution With FSI
Mode 1	169.70	63.64

Table 15. Comparison of Natural Frequency with and without FSI for Mode 1 Initial Displacement with Impulse Load.

6. Mode 2 Displacement as Initial Conditions without Load—With and Without FSI

Figure 40. and Figure 41. are the frequency spectra of a clamped-clamped beam with and without FSI, respectively, when the beam had the second mode shape as the initial condition without any external load applied to it during the simulation.

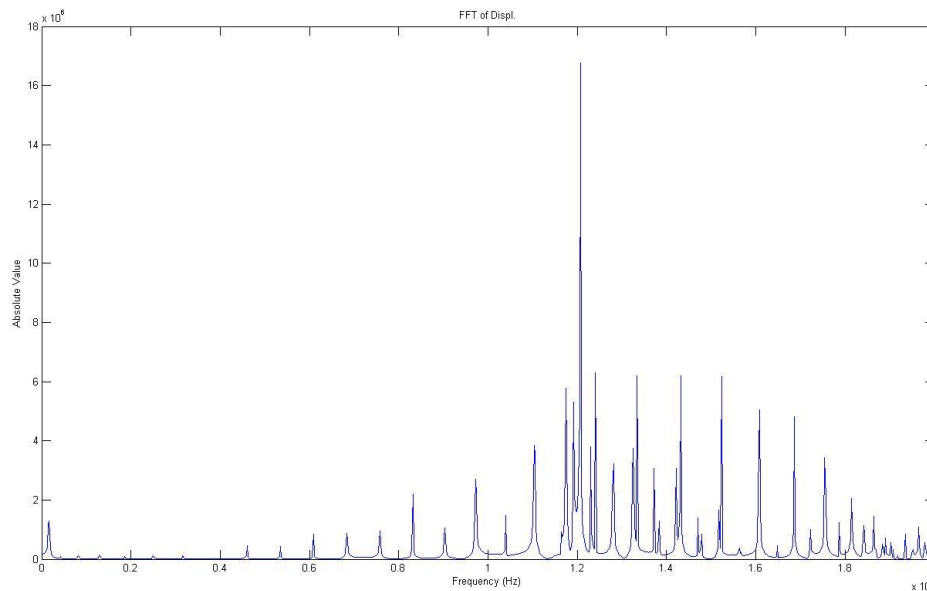


Figure 40. FFT of Displacement, without FSI.

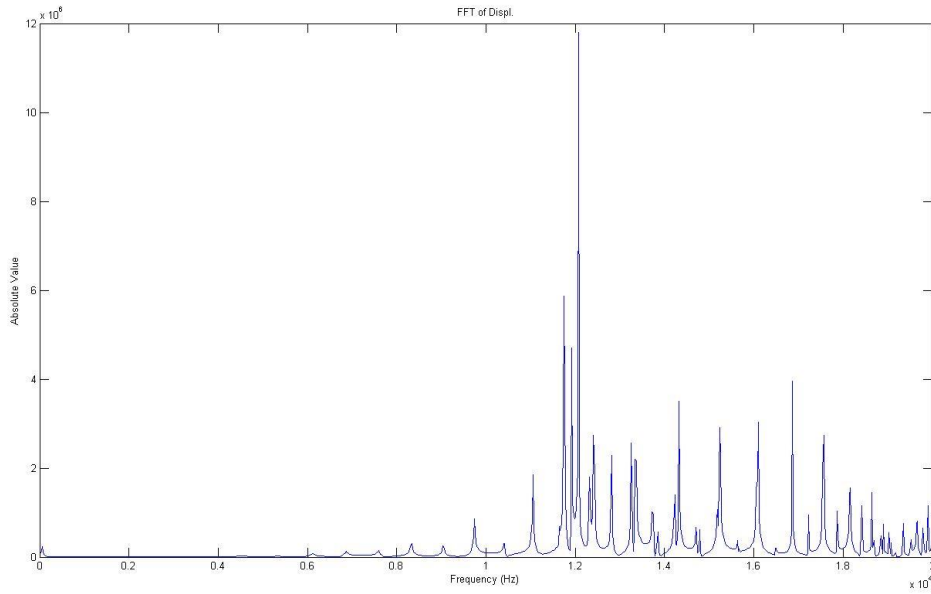


Figure 41. FFT of Displacement, with FSI.

Table 16 shows the natural frequency of the first mode of the beam for this case. All frequencies are in Hz.

	Natural Frequency Transient Solution Without FSI	Natural Frequency Transient Solution With FSI
Mode 1	169.70	63.64

Table 16. Comparison of Natural Frequency with and without FSI for Mode 2 Initial Displacement.

7. Mode 2 Displacement as Initial Conditions with Impulse Forcing Load—With and Without FSI

Table 17. shows the natural frequency of the first mode of the beam that was calculated from the program for the case where fluid-structure interaction was included and the fluid was water. The initial condition was that the beam had as initial displacement the analytical solution for the deflection of mode shape 2. In this case an impulse forcing load was applied. All frequencies are in Hz.

	Natural Frequency Transient Solution Without FSI	Natural Frequency Transient Solution With FSI
Mode 1	169.70	63.64

Table 17. Comparison of Natural Frequency with and without FSI for Mode 2 Initial Displacement with Impulse Load.

8. Mode 3 Displacement as Initial Conditions without Load—With and Without FSI

Figure 42. and Figure 43. are the frequency spectra of a clamped-clamped beam with and without FSI, respectively, when the beam had the third mode shape as the initial condition without any external load.

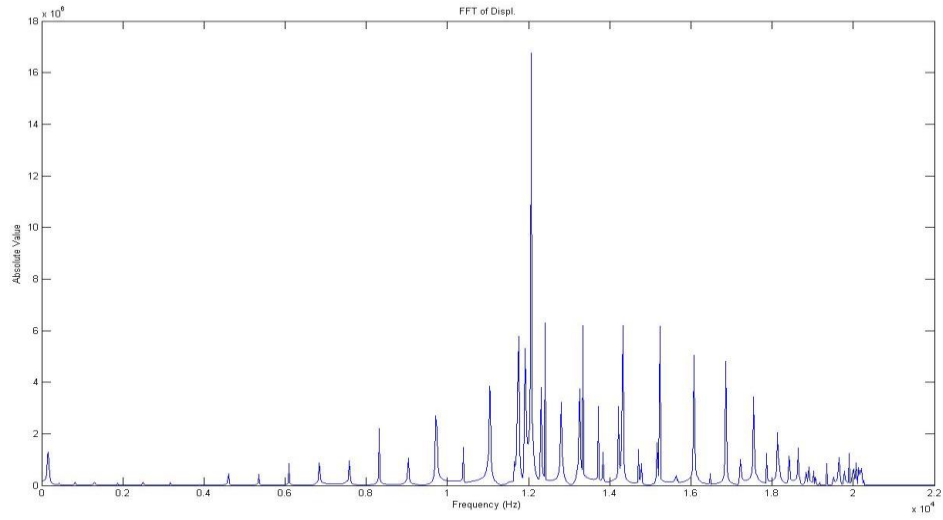


Figure 42. FFT of Displacement, without FSI.

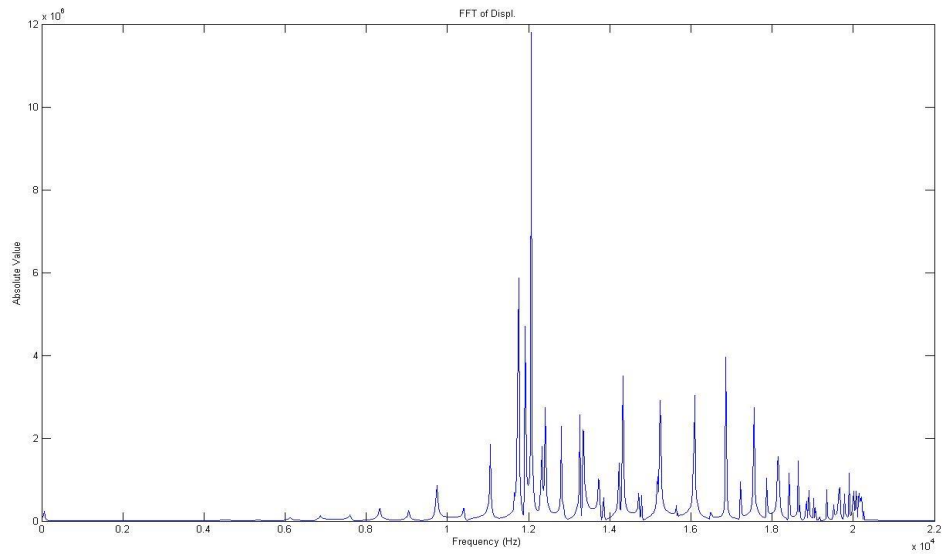


Figure 43. FFT of Displacement, with FSI.

Table 18 shows the natural frequency of the first mode of the beam for this case. All frequencies are in Hz.

	Natural Frequency Transient Solution Without FSI	Natural Frequency Transient Solution With FSI
Mode 1	169.70	63.64

Table 18. Comparison of Natural Frequency with and without FSI for Mode3 Initial Displacement.

9. Mode 2 Displacement as Initial Conditions with Impulse Forcing Load—With and Without FSI

Table 19. shows the natural frequency of the first mode of the beam that was calculated from the program for the case where fluid-structure interaction was included and the fluid was water. The initial condition was that the beam had as initial displacement the analytical solution for the deflection of mode shape 3. In this case an impulse forcing load was applied. All frequencies are in Hz.

	Natural Frequency Transient Solution Without FSI	Natural Frequency Transient Solution With FSI
Mode 1	169.70	63.64

Table 19. Comparison of Natural Frequency with and without FSI for Mode 3 Initial Displacement with Impulse Load.

C. SUMMARY OF COMPOSITE BEAM FEM INCLUDING FSI

The solution of the beam FSI problem was implemented by solving for the eigenvalue solution. Then the analytical equations for the mode shapes were used and given as input to the Beam FEM program in order to serve as the initial conditions of the beam. This is superior to the experimental testing because in the laboratory one cannot actually ‘hold’ the actual beam deformed in, for example, mode shape 3. The FEM has a

great advantage in this case, since it can precisely and accurately computationally represent any mode shape and set it as the Initial Conditions and solve for the structure response.

Some of the findings are summarized in the following list.

- All natural frequencies of the submerged (underwater) beam were calculated to be significantly lower than those calculated when the beam was surrounded by air.
- The type and the duration of the applied forcing load played a significant role in the excitation of certain modes.
- The location where the forcing load was applied had a very significant effect on which modes were excited, as expected.
- By studying the produced plots we clearly verify that when FSI is included more energy is stored in higher vibration modes.
- The model performed excellently when comparing the mode shapes for each case of 'wet' versus 'dry'.
- We observed an 'added mass' effect as well as an additional damping effect in the case where FSI was included. The presence and the interaction of the water caused the natural frequencies of the beam to have a lower value than the 'dry' case by 51%.
- The impact type of applied forcing load had a more significant effect in air than in water. This effect was probably due to the 'more damping' phenomenon observed in the FSI case due to the presence of the water.
- The calculation results that are represented by the plots indicated that in the 'wet' case, there was a greater difference in the mode shapes of the higher modes than in the first modes.

V. COMPOSITE PLATE FINITE ELEMENT MODEL INCLUDING FLUID-STRUCTURE INTERACTION

This chapter contains the description of the 3D composite-plate finite element model that we used in order to study, calculate, and analyze the dynamic response of the plate structure. The results of the various calculations were provided using the FEM of a composite 3D plate that we have developed. It includes the summary of this part of the research. Characteristic plots of the results are presented for comparison and analyses.

A. 3D COMPOSITE-PLATE FINITE ELEMENT MODEL

The parameters of the 3D composite plate that we used in this study were:

- The 3D plate material is composite material.
- Young's modulus of elasticity $E=20\text{GPa}$.
- Poisson's ratio $\nu=0.30$.
- Plate's density $\rho=2000\text{ kgr/m}^3$.
- Plate's length=1m.
- Plate's width=1m.
- Plate's depth (or thickness)=0.02 m.
- The fluid is assumed to be water. It is assumed that there is no fluid flow and no viscosity in the fluid medium.
- Water density= 1000kgr/m^3 .
- Speed of sound in the fluid medium is $c=1500\text{m/sec}$.
- The boundary conditions of the plate are clamped at all sides.

Several different initial conditions and loading states were simulated in this study. Initially the plate had zero displacement over its whole area as initial conditions while an impact load was applied for a very short time interval. For the next study, we applied the statics solution for the central force or moment as an initial condition of the plate. The results of the calculations, the plots of the mode shapes, the deformed surface, and some characteristic 'snapshots' of several time steps are presented here. Figure 44. shows the finite element mesh of the plate element.

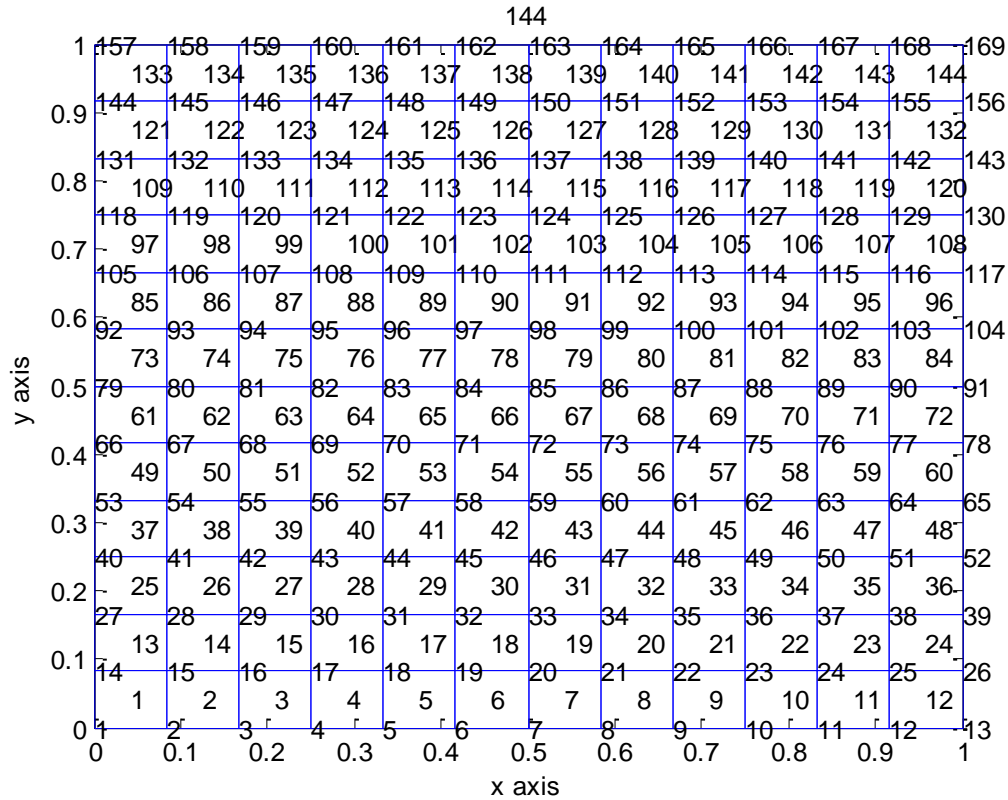


Figure 44. Mesh of the 12X12 3D FEM Plate.

B. RESULTS OF PLATE FEM CALCULATION INCLUDING FSI

The results that we acquired from the FEM program were simulating different loading and initial conditions for the 3D composite plate and are divided into the following cases.

1. Statics Solution (Produced by Forcing Load) as Initial Conditions without Applied Load

The first calculation of the dynamic response of the 3D composite plate was done with the initial conditions to be the static deformation caused by a force applied to the center of the plate. This statics solution of the plate was obtained using the FEM program, and the maximum deflection matched the analytical solution. The nodal displacements of the statics solution were loaded onto the FEM program as initial conditions. Then we calculated the dynamic response of the plate with and without FSI.

Figure 45. shows the static deflection used as the initial condition. Figure 46. and Figure 47. compare the vibrational shapes of the composite plate with and without FSI, respectively. The two plots were selected at the same vibrational time.

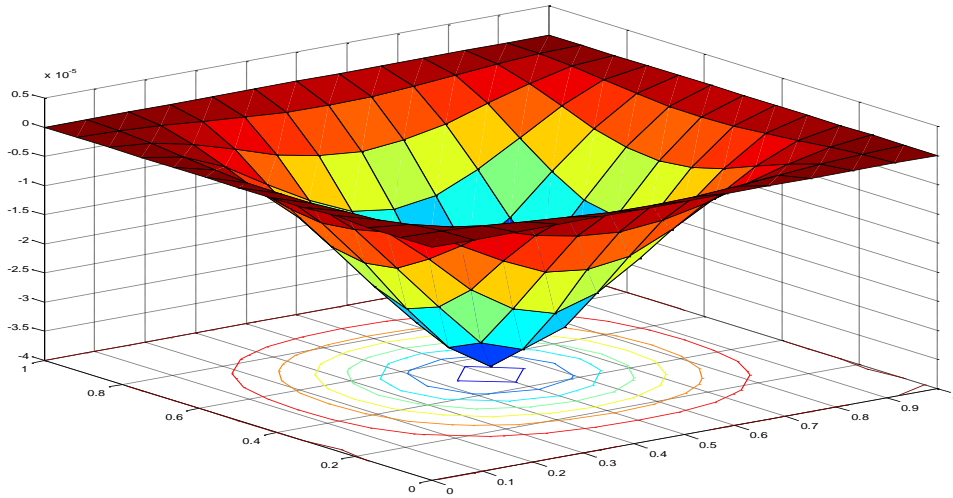


Figure 45. Initial Conditions of 3D Plate for this Case.

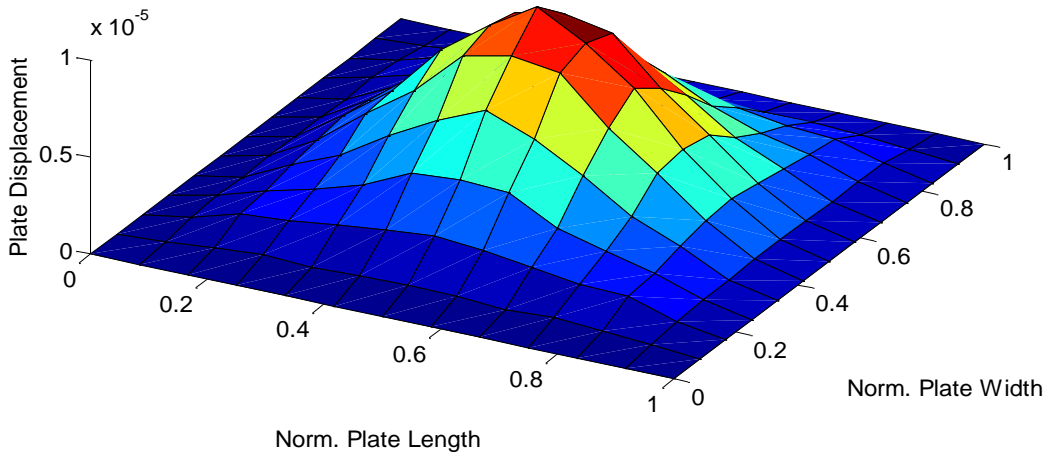


Figure 46. Overall Surface of Deformed Plate, without FSI.

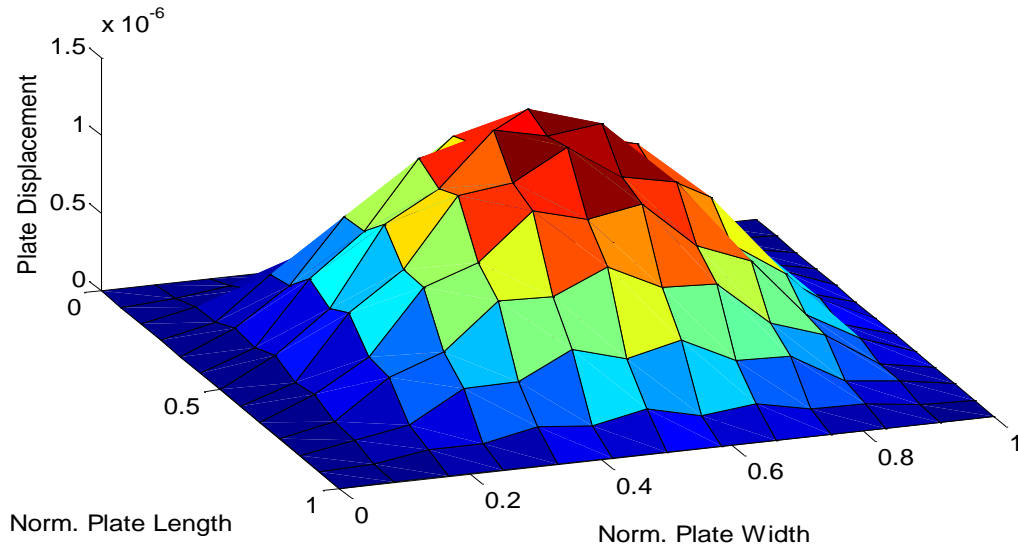


Figure 47. Overall Surface of Deformed Plate, with FSI.

We see that when the FSI is included in the calculations, a different vibration mode is excited. By examining the deformation of the plate and by using the FFT technique we also notice that higher modes have already started to show up in the FSI case, while this does not occur in the non-FSI case.

Plotting the deformed surface of the 3D composite plate at a later time step, we have the same findings as before. In this case, the higher frequency modes have already started to affect significantly the plate vibration characteristics as compared to the results shown in Figure 48. and Figure 49. .

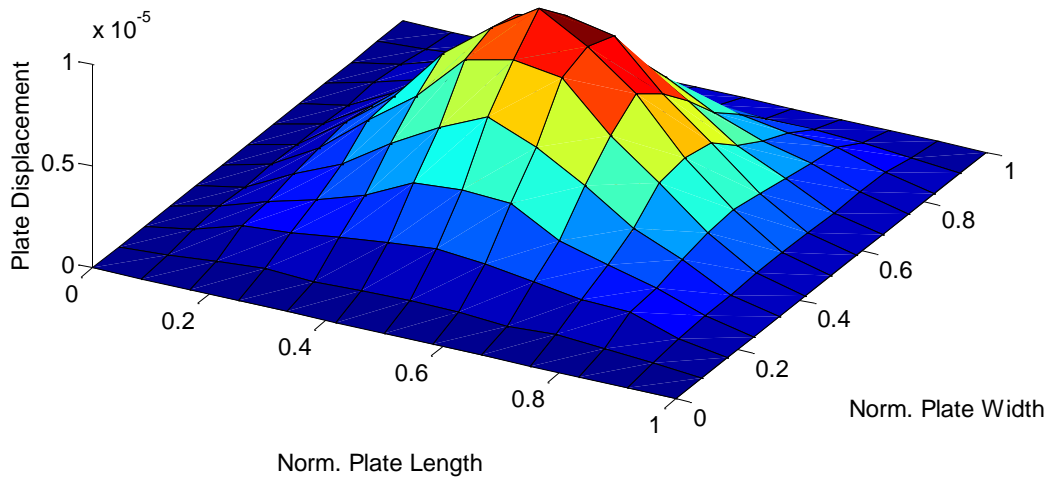


Figure 48. Deformed Plate, without FSI.

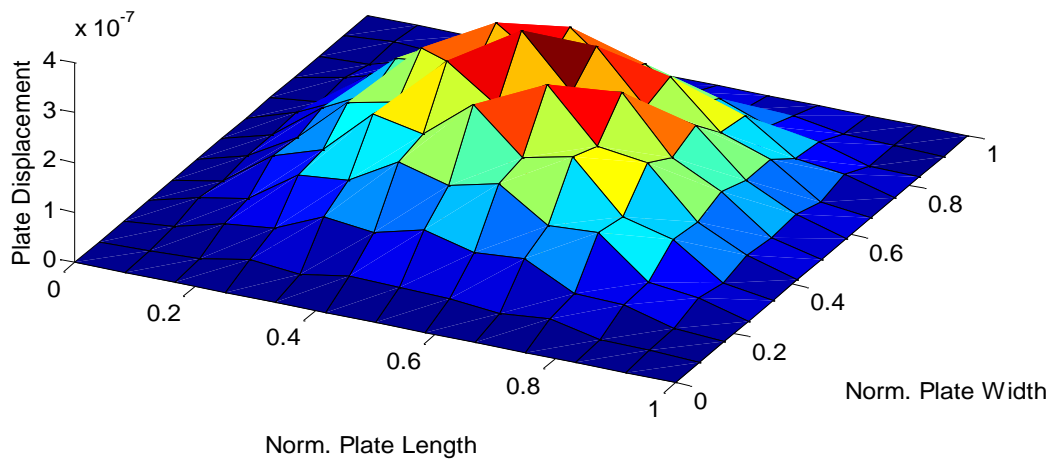


Figure 49. Deformed Plate, with FSI.

We used the fast Fourier transform inside our program to verify that our finding about the plate's response was indeed true. The FFT calculation of the displacement of the plate supported our observation. The FFT plots are shown in Figure 52. and Figure 53. .

From the FFT, we compared the first mode shape of the plate with and without FSI, respectively, as shown in Figure 50. and Figure 51. .

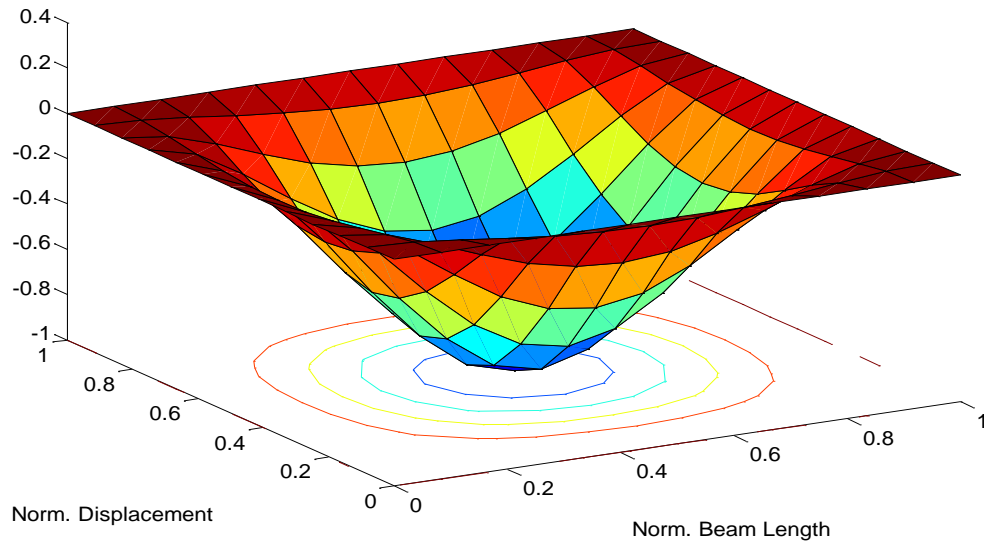


Figure 50. Mode One, without FSI.

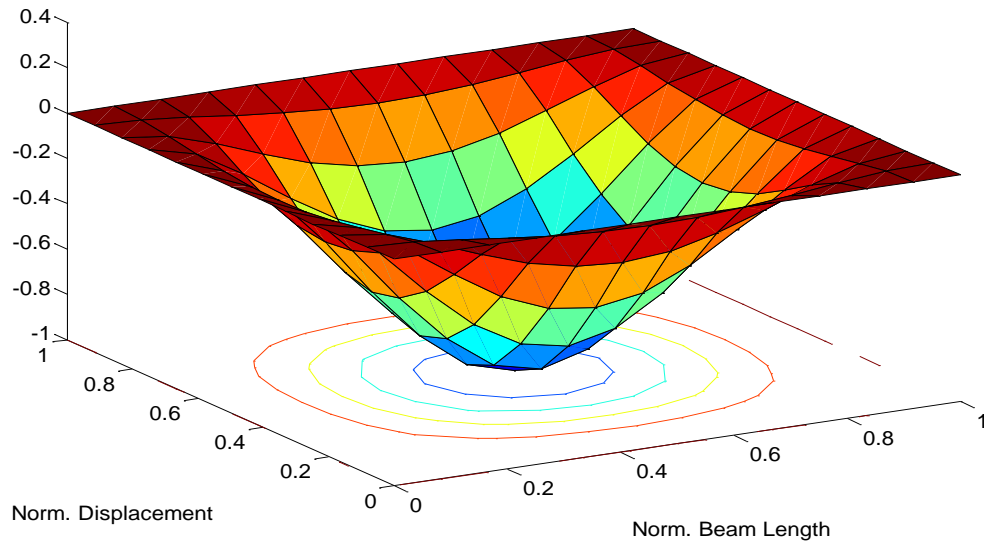


Figure 51. Mode One, with FSI.

The plots of the calculation results from the FFT of the displacement of the central node of the plate are shown in Figure 52. and Figure 53. .

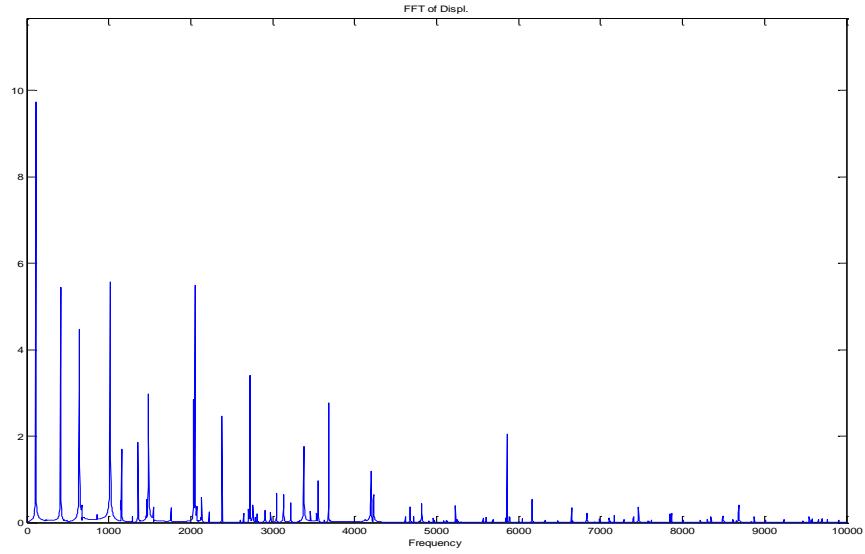


Figure 52. FFT of Displacement, without FSI.

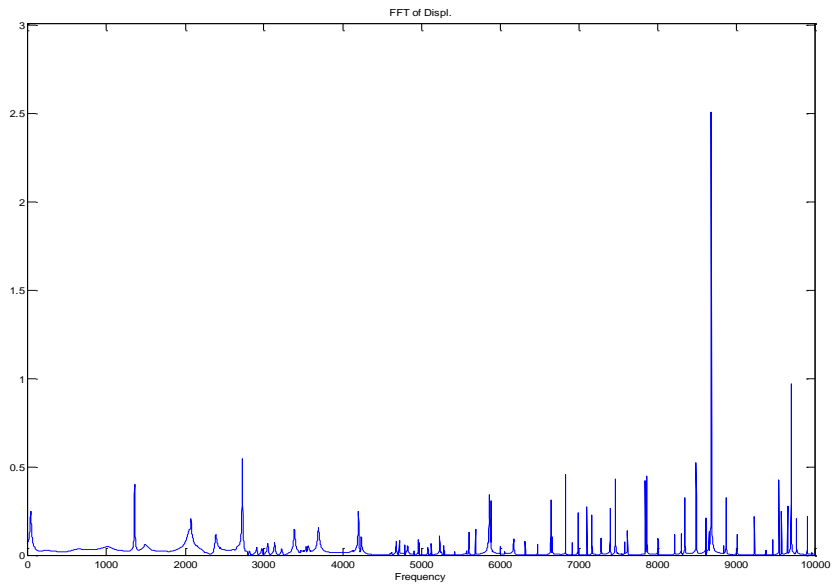


Figure 53. FFT of Displacement, with FSI.

From these results we clearly see that the FSI case excites higher frequency mode shapes. Therefore, more energy is stored in the higher frequencies. This plays a significant role in the dynamic response of the plate as the curvatures are also affected and so the bending strain at the affected nodes will alter the failure modes of the plate.

2. Zero Displacement as Initial Conditions with Impact Forcing Load— With and Without FSI

In this case we chose the initial conditions of the plate to be zero displacement. That means that the plate had zero displacement at every nodal point before the FEM program ran. The load was computationally applied for a very short time interval. The load was an impact force acting on the displacement dof of the node at the center of the plate. We chose forcing load to simulate impact conditions on the composite plate.

The program ran for 6,000, 10,000, and 12,000 time steps, and after completion we computed the FFT of the displacement so as to monitor the natural frequencies that were excited the most. If the mode shapes were not changed due to FSI, the difference should be zero or at least negligible.

The resulting plots include 3D ‘snapshots’ of the deformed plate with and without FSI at the same time step for comparison, as seen in Figure 54. and Figure 55. The displacement of the center node of the plate is plotted over time and presented for each case. Figure 56. and Figure 57. show the time history of the central displacement of the plate. Finally, the FFT of the displacement is calculated and plotted in Figure 58. and Figure 59. in order to observe the behavior of the structure and to monitor and verify the ‘distribution’ of the energy going into the vibration of the plate.

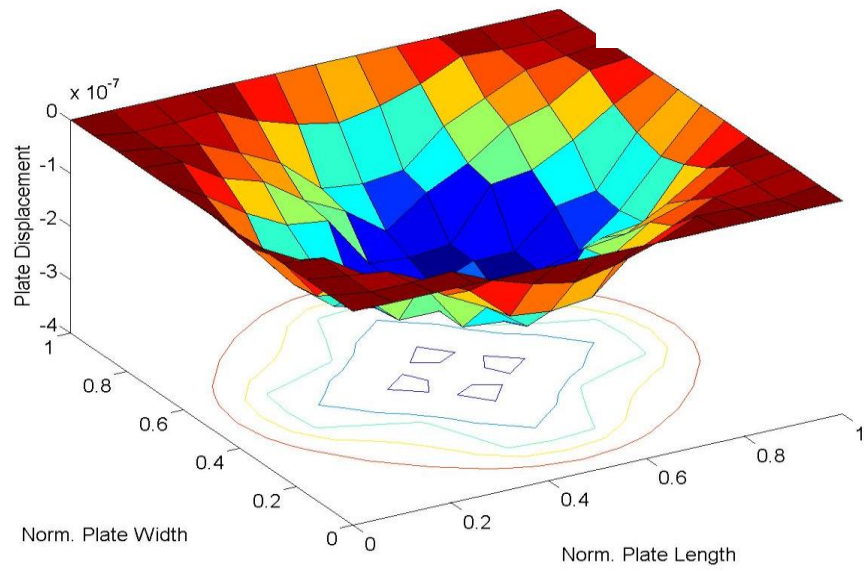


Figure 54. Deformed Plate, without FSI.

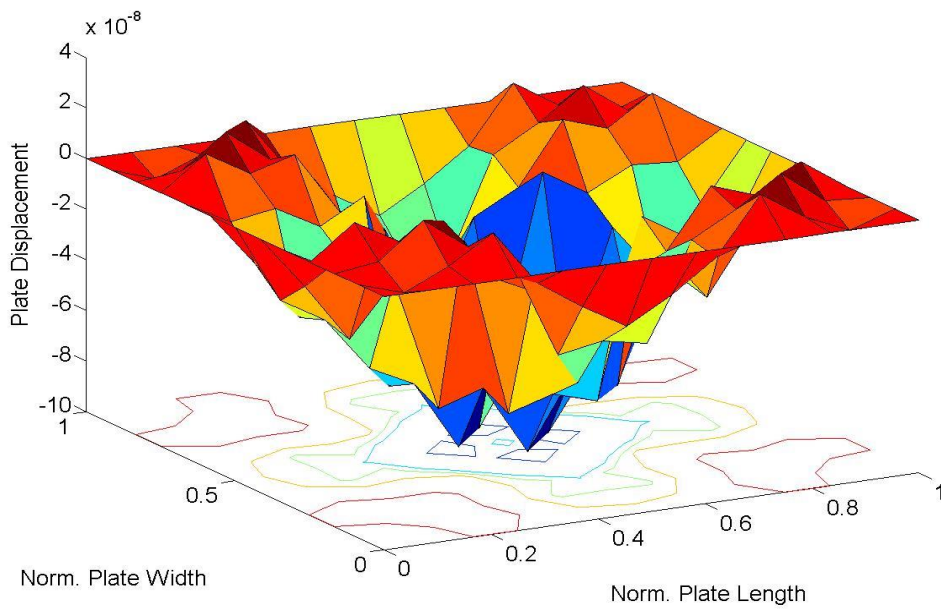


Figure 55. Deformed Plate, with FSI.

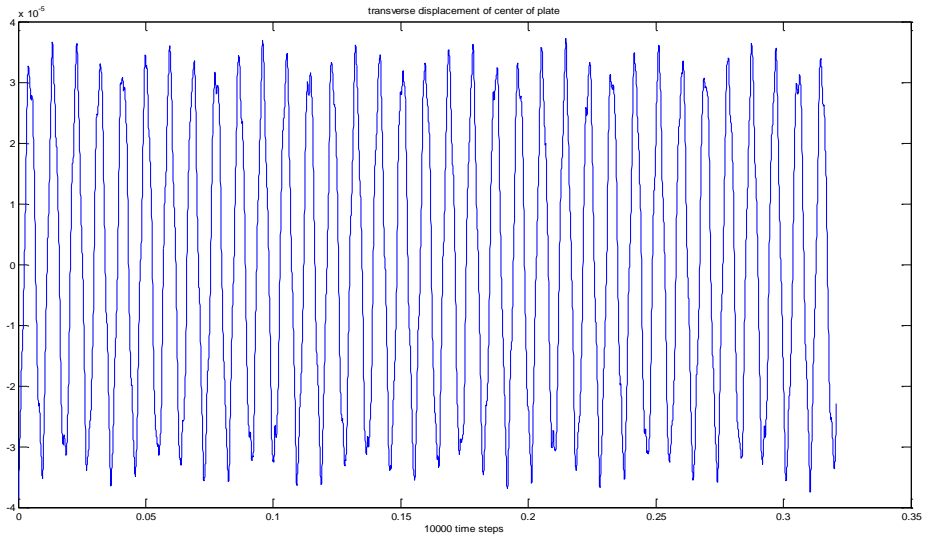


Figure 56. Displacement of Central Node, without FSI.

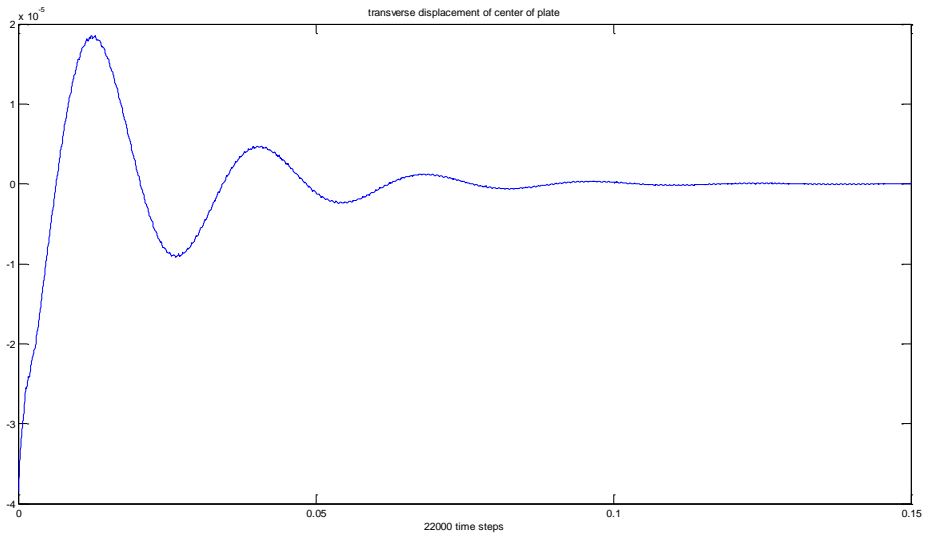


Figure 57. Displacement of Central Node, with FSI.

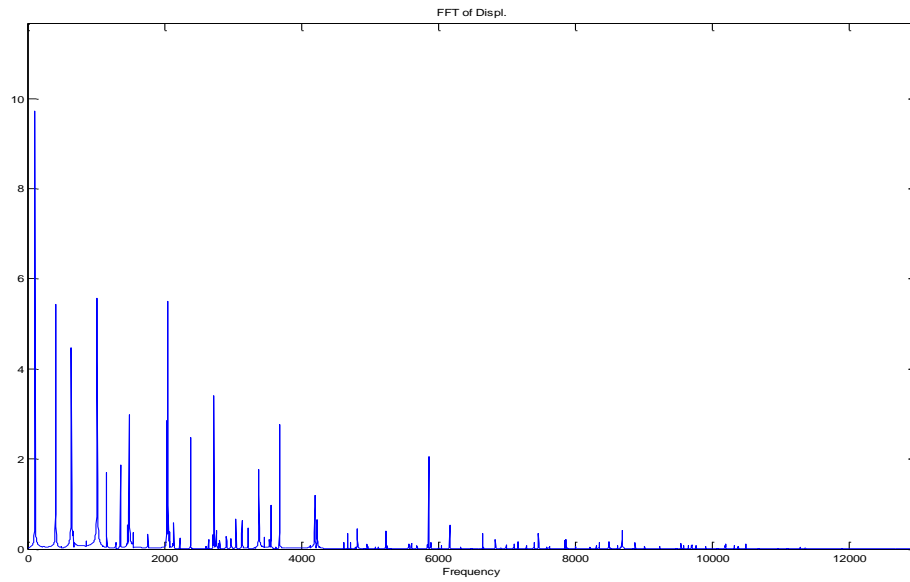


Figure 58. FFT of Displacement, without FSI.

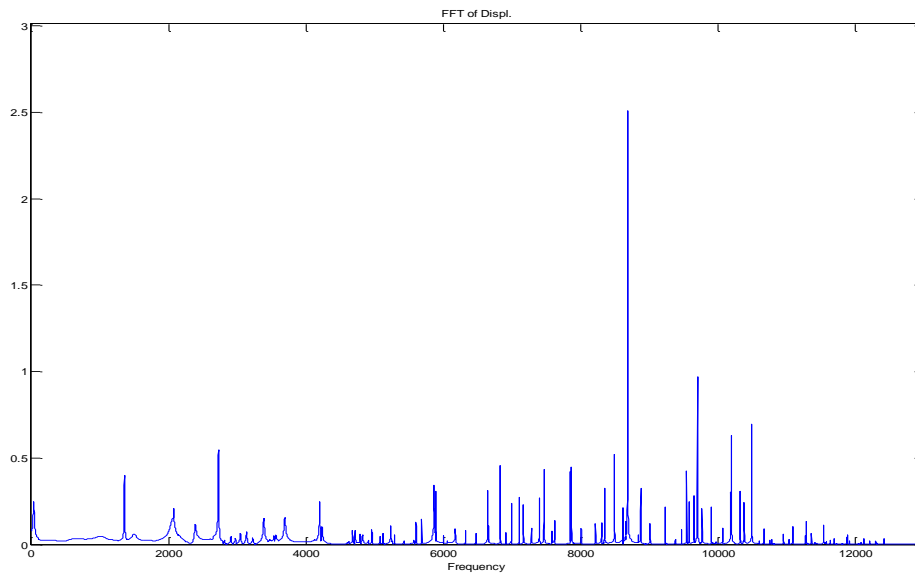


Figure 59. FFT of Displacement, with FSI.

Then, we plot the first mode for the cases with and without FSI for this simulation case (Figure 60. and Figure 61.).

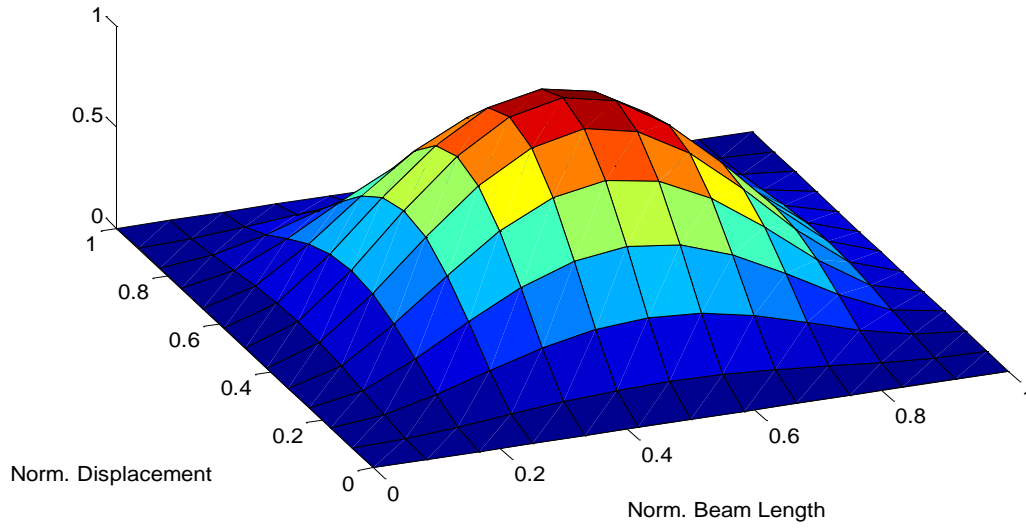


Figure 60. Mode One, without FSI.

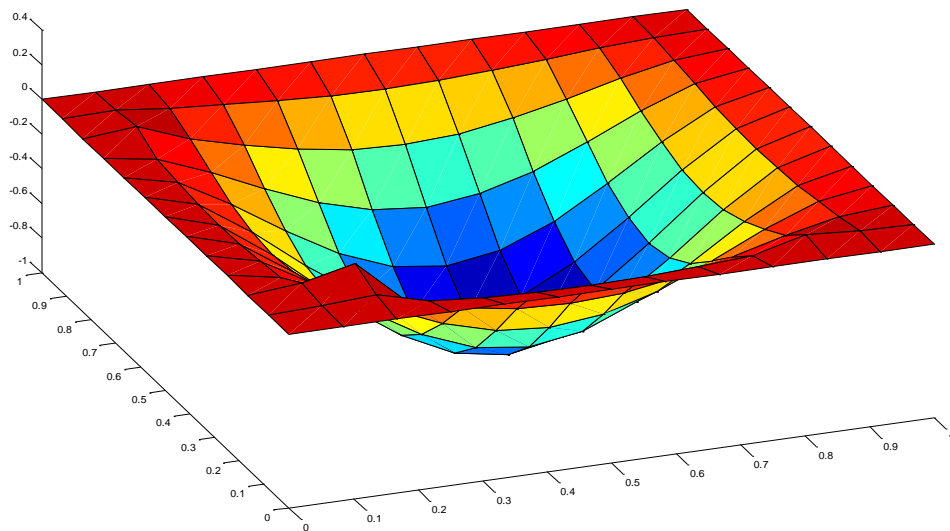


Figure 61. Mode One, with FSI.

We computed the difference of the first mode shape between the non-FSI and the FSI case, and we plotted the difference in Figure 62. .

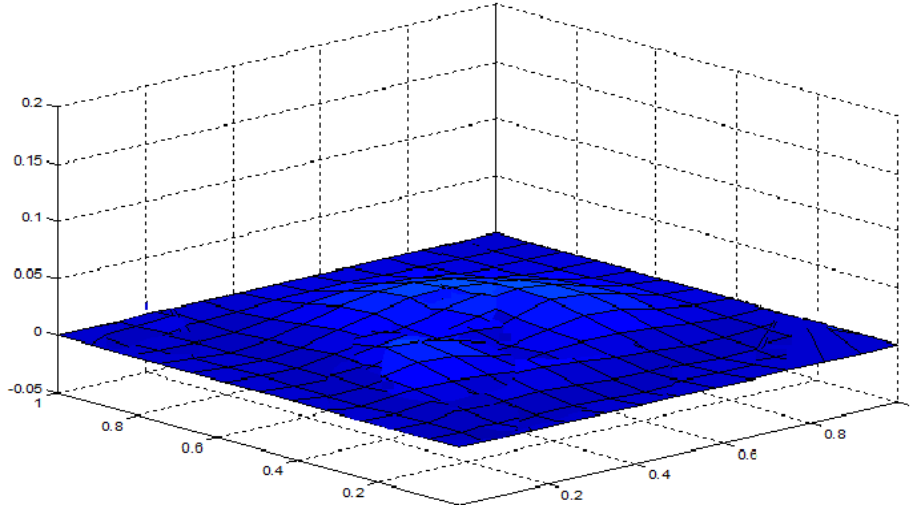


Figure 62. Mode One Difference, without-with FSI.

The plot of the next mode shape is provided in Figure 63. for the non-FSI case, whereas the plot of the same mode for the FSI case is shown in Figure 64. . Because the impulse load was applied at the center, the numerical modal analysis could not obtain non-symmetric mode shapes. As a result, the mode shape shown in Figure 63. and Figure 64. are not the second mode shape of a clamped square plate.

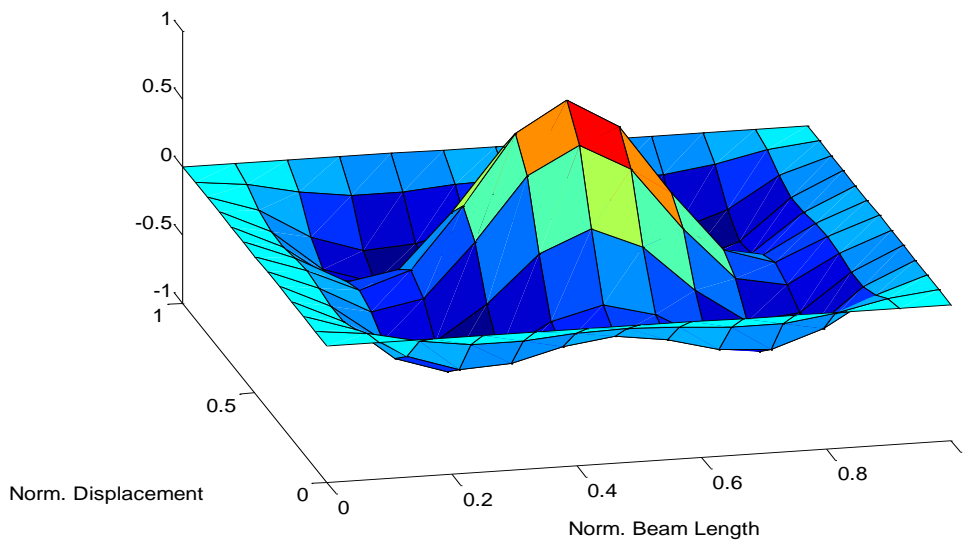


Figure 63. Second Symmetric Mode, without FSI.

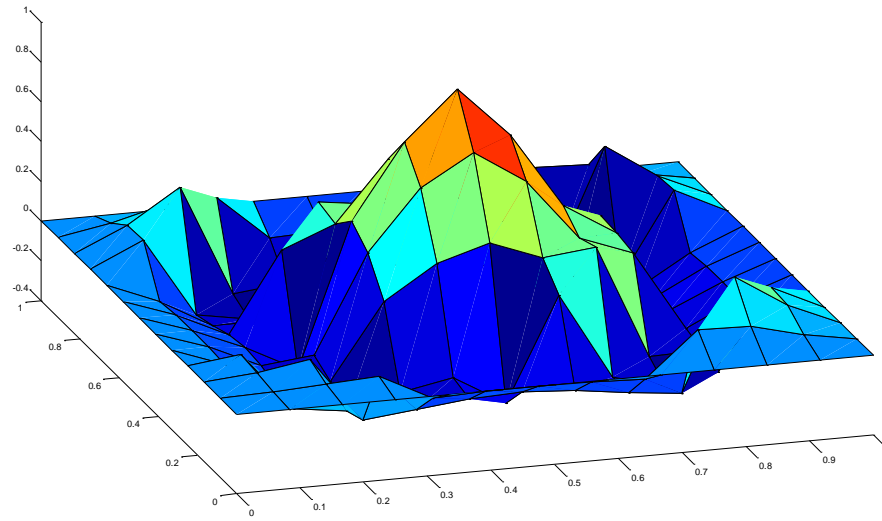


Figure 64. Second Symmetric Mode, with FSI.

The difference in the nodal displacements of the second mode shape between the non-FSI and the FSI cases was calculated and plotted in Figure 65. .

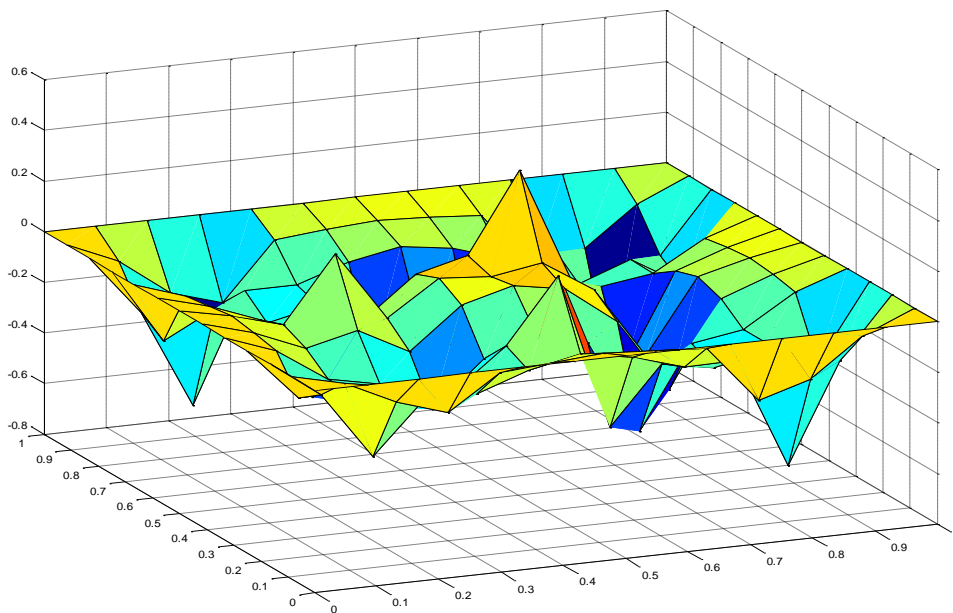


Figure 65. Second Symmetric Mode Difference, without-with FSI.

3. Statics Solution (Produced by Moment Load) as Initial Conditions— With and Without FSI

The initial conditions were chosen to be the statics solution for the deflection of the plate when subjected to a moment load on the center node of the plate. This statics solution was calculated using the Ex1092 [2] finite element program since the analytical/exact solution for this case is not known. The initial displacement of the plate is plotted in Figure 66. .

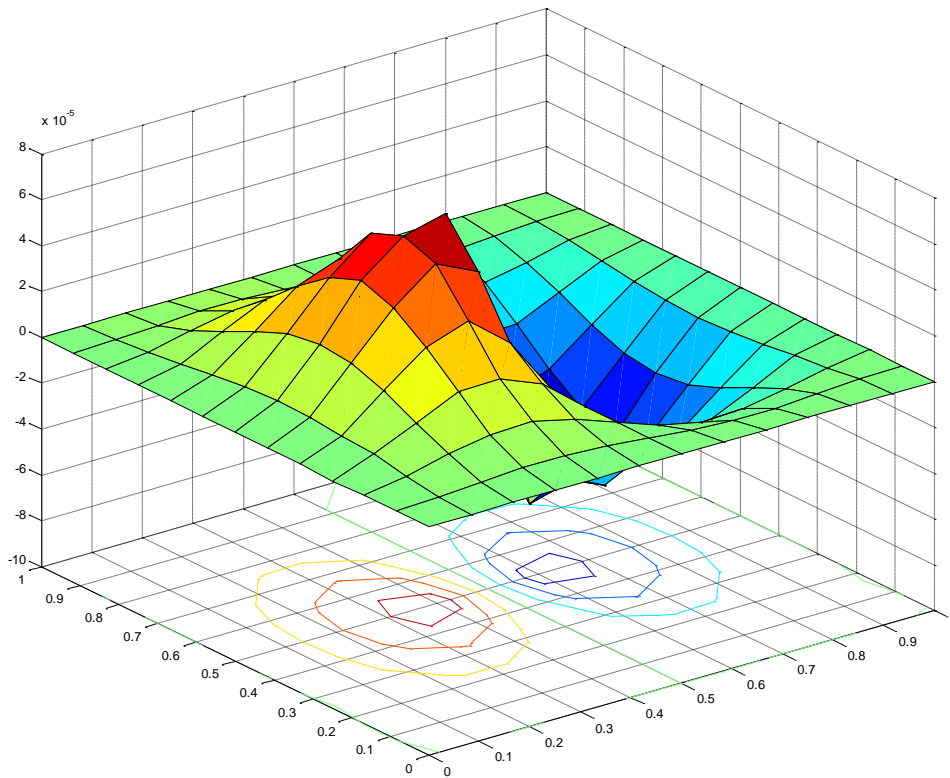


Figure 66. Initial Conditions for this Case.

In Figure 67. and Figure 68. the overall deformed surface of the vibrating composite plate is shown for the non-FSI and the FSI cases. The plots were created for the same, but arbitrarily selected, time instant (time step).

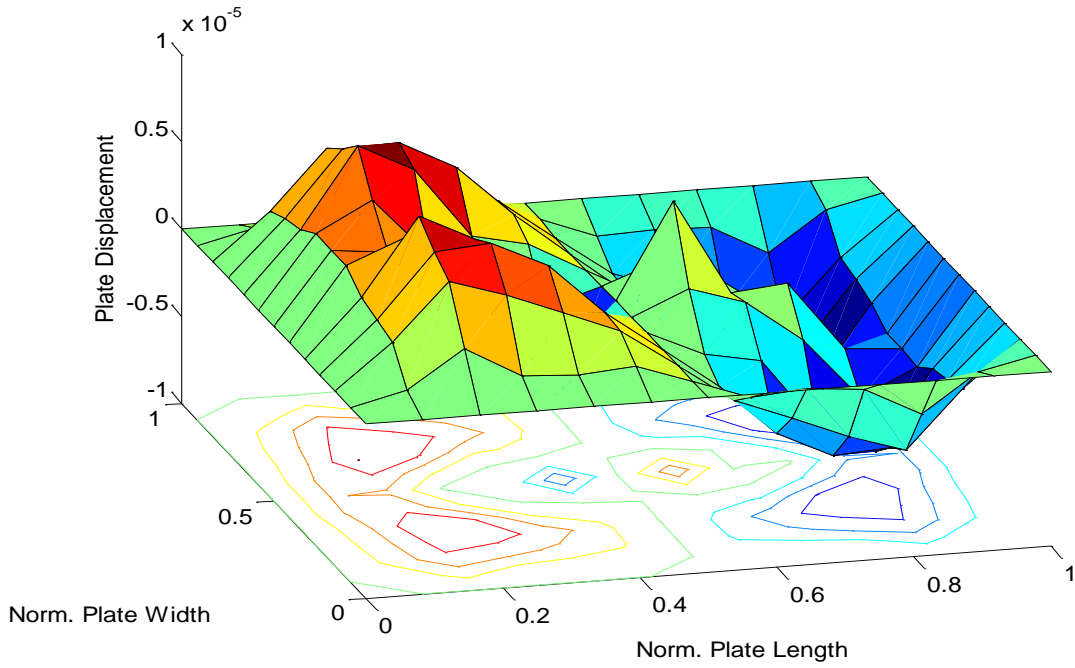


Figure 67. Deformed Plate, without FSI.

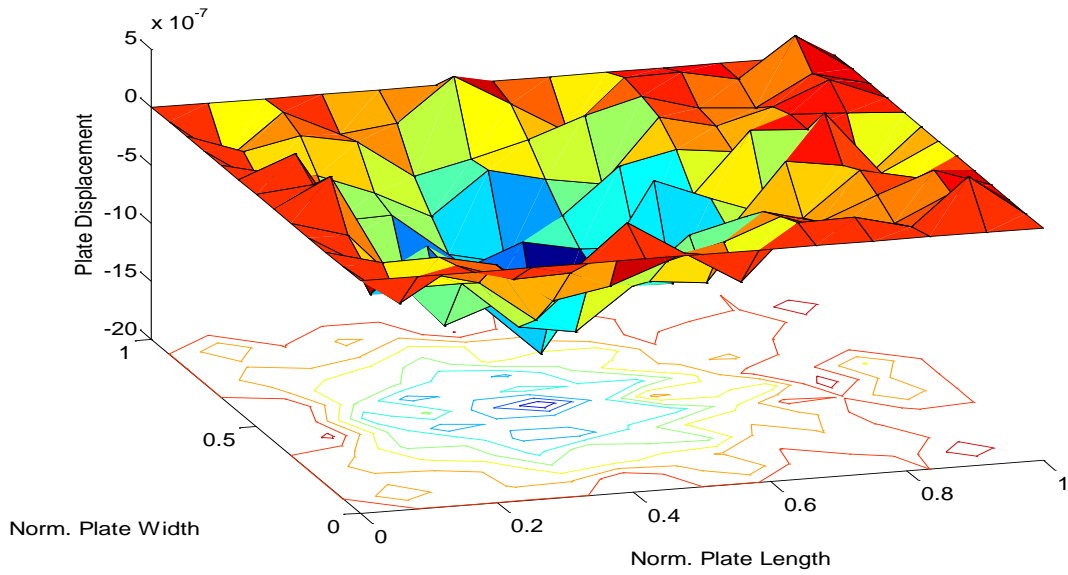


Figure 68. Deformed Plate, with FSI.

Figure 69. and Figure 70. are the plots of the displacement of the node at the center of the plate.

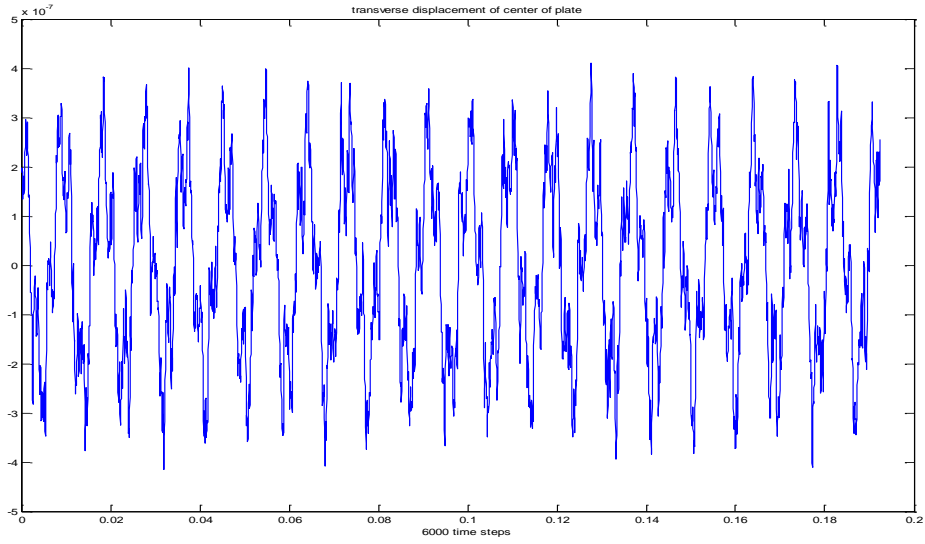


Figure 69. Displacement at Center Node, without FSI.

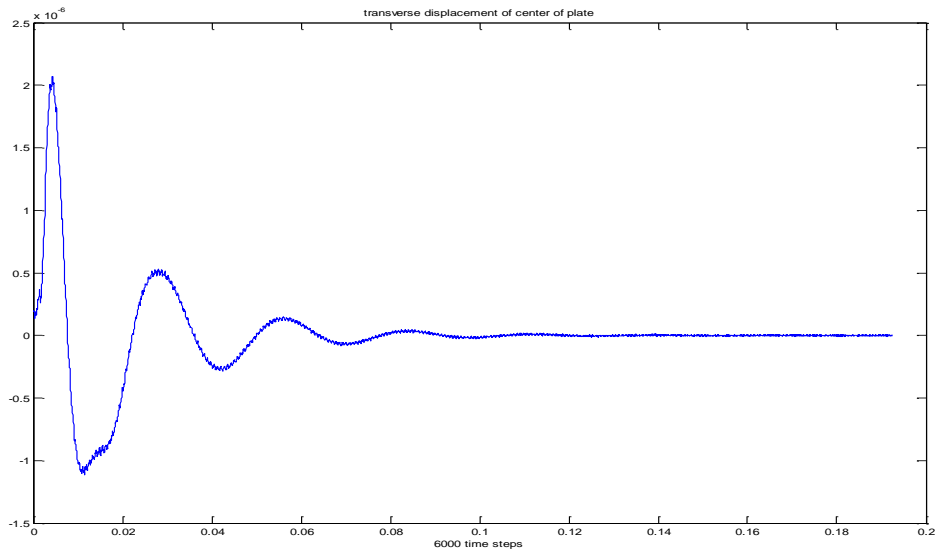


Figure 70. Displacement at Center Node, with FSI.

In Figure 71. and Figure 72. we have plotted the FFT of the displacement of the central node of the plate for the non-FSI and for the FSI cases.

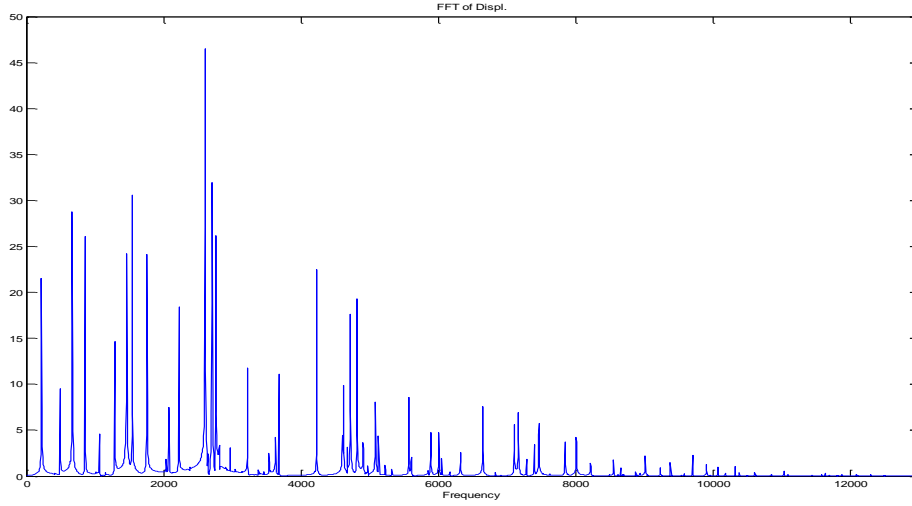


Figure 71. FFT of Displacement, without FSI.

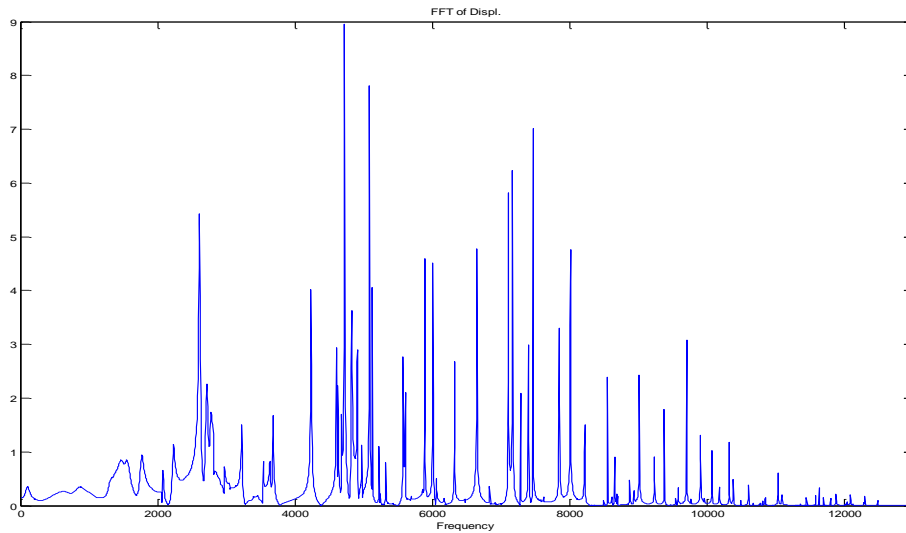


Figure 72. FFT of Displacement, with FSI.

From the plots in Figure 73. and Figure 74. , we can see the same mode shape for the non-FSI and the FSI cases.

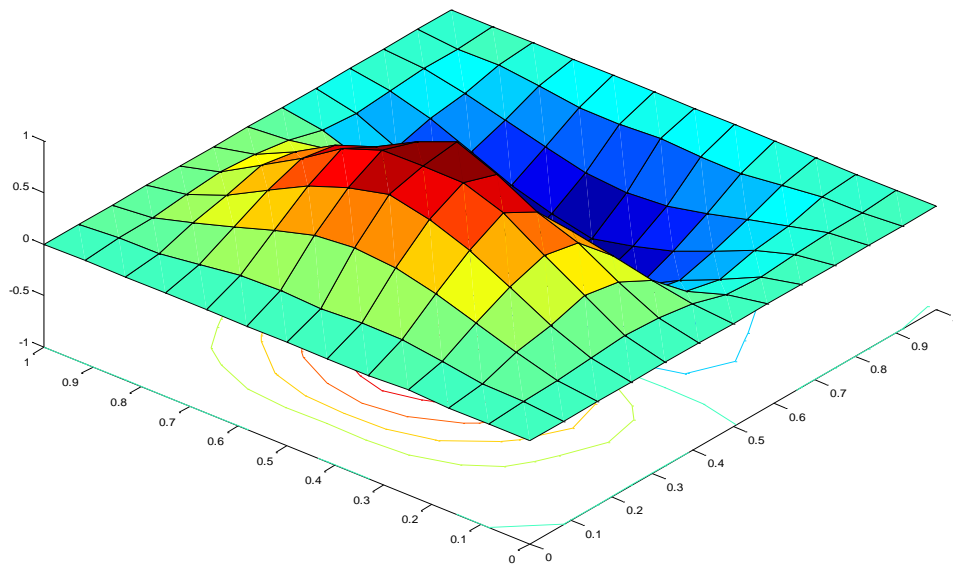


Figure 73. Mode Shape, without FSI.

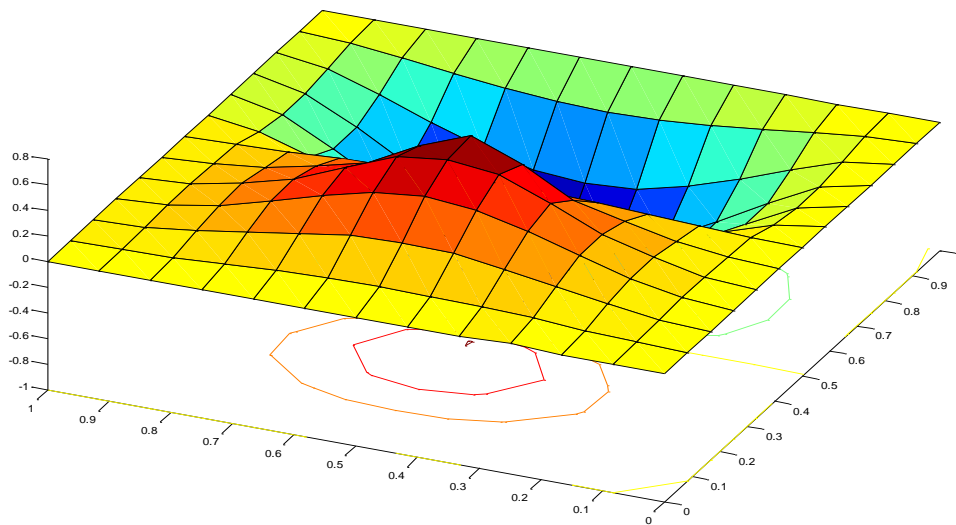


Figure 74. Mode Shape, with FSI.

Figure 75. shows the difference of the nodal displacements of the same mode shape between the non-FSI and the FSI cases.

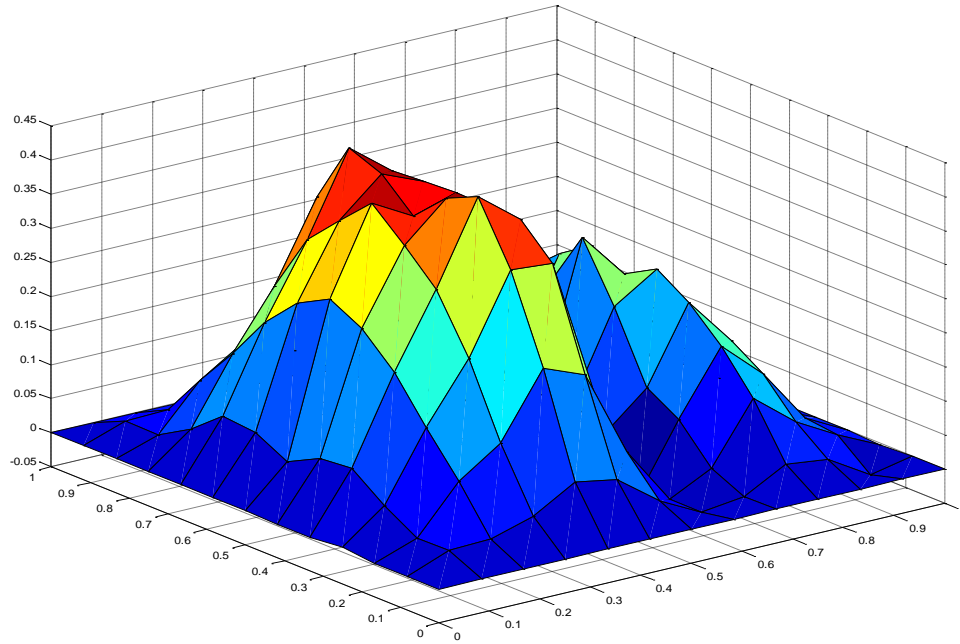


Figure 75. Mode Shape Difference, without–with FSI.

In Figure 76. and Figure 77. the next mode shapes of the composite plate are compared for the non-FSI and the FSI cases. Figure 76. and Figure 77. are very close to Figure 73. and Figure 74. , respectively, because the plate is square and there are two identical second and third mode shapes about x- and y-axis, respectively.

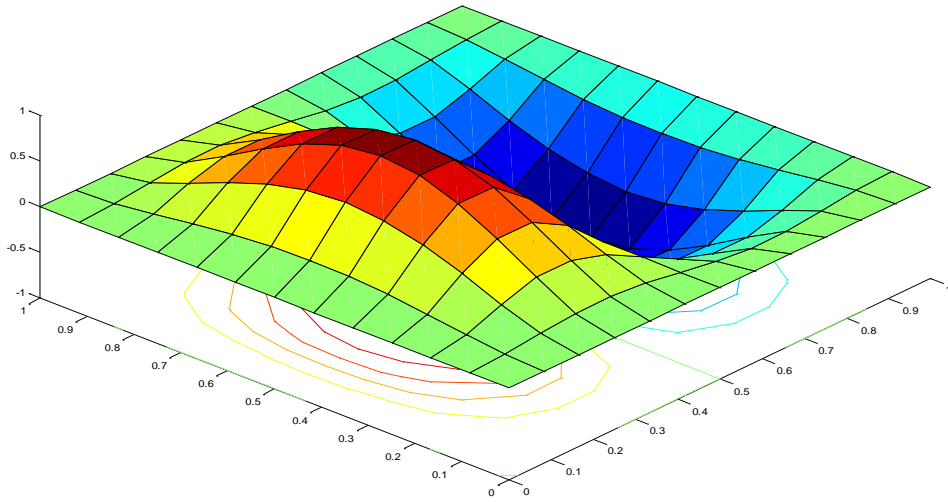


Figure 76. Mode Shape, without FSI.

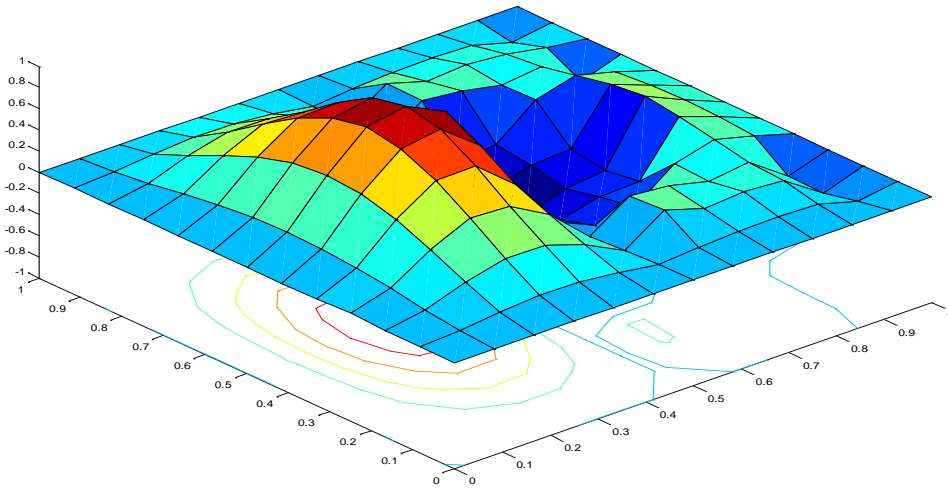


Figure 77. Mode Shape, with FSI.

Figure 78. shows the difference of the nodal displacements of the same mode shape between the non-FSI and the FSI cases.

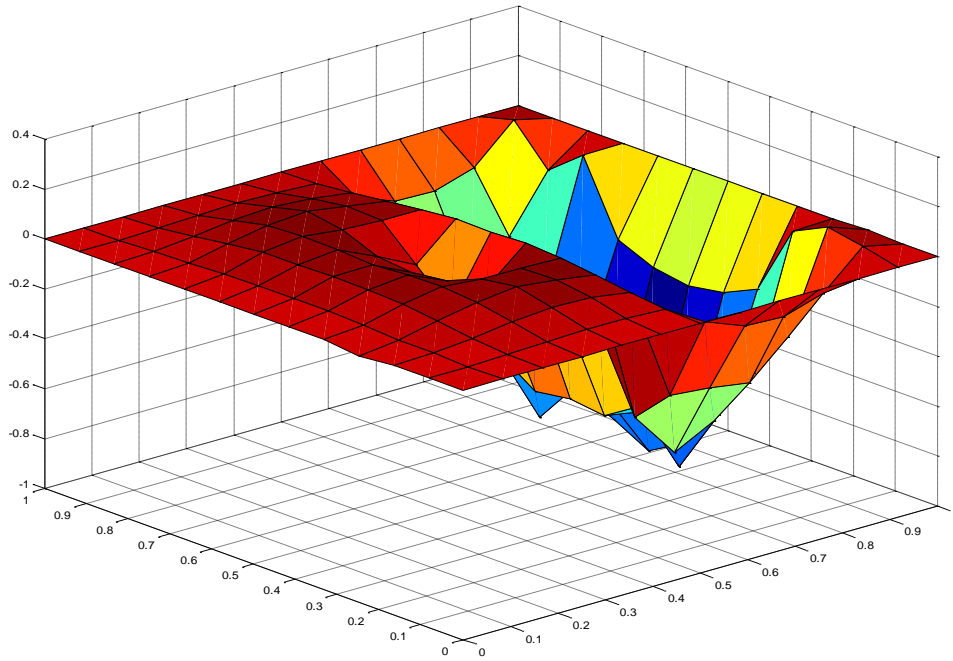


Figure 78. Mode Shape Difference, without–with FSI.

C. SUMMARY OF PLATE FEM INCLUDING FSI

Summarizing this chapter, we found that the presence of fluid has a very significant effect on the vibration characteristics of the 3D composite plate. The mode shapes and the total deformed surface of the plate is different in the FSI case than in the non-FSI case.

We observed that higher vibration modes are excited when FSI is included. The curvatures and slopes are different for the FSI case. So the possible ‘failure region’ of the composite structure is going to occur at different locations. This happens because the behavior of the plate changes due to the effect of the fluid in which the plate is submerged.

We proved that we can easily use any deformation or mode shape of the plate as initial conditions for the plate. This is a most significant advantage of the computational method as compared to the experimental method, since during the actual experiment the plate sample cannot be held in any mode shape or deformation pattern that we arbitrarily choose. While using the FEM for the simulation and analysis of the plate, we can virtually 'hold' the structure in any shape that we wish to use as initial conditions. For example, experimentally applying moment on a specific dof is a technical challenge. But using the FEM program we can apply moment on any rotational dof that we wish to choose.

THIS PAGE INTENTIONALLY LEFT BLANK

VI. CONCLUSIONS AND RECOMMENDATIONS

The finite element model of the structures studied here provides a handful of very useful results and insights related to the dynamic analysis and simulation of the composite structures.

A. SUMMARY OF CONCLUSIONS

There are great advantages in using computational methods in order to study, explore, and calculate the dynamic response of structures. We do not need to actually build an experimental structure in order to iterate and optimize the objective structure. Therefore, the cost of engineering design is much lower than the cost of using exclusively experimental samples that have to undergo extended and time-consuming experiments. The actual model or experimental sample will be built and tested, only after it has been studied, analyzed, and optimized through the FEM program. That way much fewer samples need to be built, less testing time will be needed, and therefore the cost is significantly less. However, the finite element method offers only a brief insight into what the actual structure behavior will be, because there are some discrepancies between the real structures and the finite element models.

The FEM program that we used to study the 2D composite beam was validated by comparing the solutions for the natural frequencies, the mode shapes, and the deformed surface of the beam, with the analytical ones. The two sets of solutions were found to be either almost equal or very close. The more finite elements we used, the more accurate the FEM solution proved to be, but more computational time was needed to complete the calculations, as expected. The vibration modes with lower natural frequencies were more accurately represented by the FEM program than higher frequencies and corresponding modes.

The study of the 2D composite beam showed clearly that the presence of the fluid (i.e., in our case the water) had a significant effect on the behavior of the structure. It changed the vibrational characteristics of the beam. When FSI was included, higher vibration/frequency modes were excited. More energy was ‘stored’ in higher modes and

higher natural frequencies were excited. This has a serious ‘impact’ on the structural integrity of the beam because the curvature of the beam is directly related to its bending strain. Therefore, special care must be given in any mechanical design of composite structure that involves FSI since the actual failure modes will shift and the failure locations will change significantly when the FSI effect is present as compared to the non-FSI case.

The computational analysis of the 2D beam using different materials, such as steel and aluminum beams, also showed a significant effect when FSI was present. However, the FSI effect was much more noticeable and more active in the composite material case. This is explained due to the density of the composite material being very close to the density of water.

The FEM program that we used to computationally test the 3D composite plate was validated by comparing the solutions for the natural frequencies and the mode shapes.

The FEM program for the 3D composite plate clearly showed that when FSI was included in the simulation, higher frequencies were excited and energy was stored in higher vibration modes.

We observed an ‘added mass’ effect as well as an additional damping effect in the case where FSI was included. The presence and the interaction of the water caused the natural frequencies of the beam to have a lower value than the ‘dry’ case. Although this was the case, higher frequencies were excited due to the FSI effect.

B. RECOMMENDATIONS FOR FUTURE WORK

Future work on this subject is needed in order to further enhance the understanding of the composite material behavior. The effort must be focused on the simulation of the application of several different loading patterns and several different configurations of a structure’s supports. That way, the dynamic response of the composite structures will be further understood and evaluated.

Special attention must be given to the evaluation of the FEM results. Whether the FSI calculations using the FEM programs are providing such results due to real behavior of the structures or due to induced numerical errors that propagate throughout the iterations carried out in the FEM program is an issue that needs to be explicitly addressed and explored to a larger extent.

The results of this thesis research, as well as future results from similar research, must be compared in parallel to several experimental results for validation purposes.

Composite structures are a promising technology, especially in light of the ever growing and emerging concerns about reduced fuel consumption for naval and commercial vessel applications. But in order to safely build and use large composite vessels, we need to verify that enough research has been done to acquire safe results that will eventually lead to successfully building large naval vessels that will possess all the advantages of the composite material structures.

THIS PAGE INTENTIONALLY LEFT BLANK

LIST OF REFERENCES

- [1] L. E. Craugh and Y. W. Kwon, “Coupled finite element and cellular automata methods for analysis of composite structures with fluid-structure interaction,” Ph.D. dissertation, MAE Dept., Monterey, Naval Postgraduate School, 2013, pp.125–129.
- [2] Y. W. Kwon and H. Bang, *The Finite Element Method Using MATLAB*. 2nd ed. New York: CRC Press, 2000, pp.235–303, pp.361–390.
- [3] Y. W. Kwon. (2013, Aug.). “Analysis of laminated and sandwich composite structures using solid-like shell elements.” [Online]. *J. Appl. Composite Mater.* vol. 20, no. 4, pp. 355–373. Available: doi:10.1007/s10443-012-9273-8.
- [4] Y. W. Kwon, E. M. Priest, and J. H. Gordis, *Investigation of Vibrational Characteristics of Composite Beams with Fluid-Structure Interaction*. Waltham, MA: Elsevier, 2013, pp. 273–276.
- [5] Y. W. Kwon. (2008, Jan.). “Coupling of lattice Boltzmann and finite element methods for fluid-structure interaction application.” [Online]. *J. Pressure Vessel Technol*, vol. 130, no. 1., pp. 664–666. Available: doi:10.1115/1.2826405.

THIS PAGE INTENTIONALLY LEFT BLANK

INITIAL DISTRIBUTION LIST

1. Defense Technical Information Center
Ft. Belvoir, Virginia
2. Dudley Knox Library
Naval Postgraduate School
Monterey, California